STUDY OF THE TRANSFER BETWEEN HALO ORBITS

G. GÓMEZ
Departament de Matemàtica Aplicada i Anàlisi, Universitat de Barcelona
Gran Via 585, 08007 Barcelona, Spain
A. JORBA and J. MASDEMONT
Departament de Matemàtica Aplicada I, Universitat Politècnica de Catalunya
E.T.S.E.I.B., Diagonal 647, 08028 Barcelona, Spain
C. SIMÓ
Departament de Matemàtica Aplicada i Anàlisi, Universitat de Barcelona
Gran Via 585, 08007 Barcelona, Spain

Abstract

Two methods of transfer between halo orbits of the same family are developed making use of the geometry of the phase space around these solutions and the Floquet theory for periodic orbits. The study is done for the halo orbits around the libration point L_1 of the Earth-Sun system, in the framework of the Restricted Three Body Problem. The optimal performance of the method is given. In a second step one of the methods is adapted to the real situation taking into account the influence of all the bodies of the solar system. The results obtained are compared with other strategies studied by Hiday and Howell [13], [14] .
Key words: Restricted three body problem, halo orbits, quasi-periodic orbits, Floquet theory, invariant manifolds, transfer orbits.

1 Introduction

Halo orbits in the restricted three body problem (RTBP) are spatial periodic solutions which bifurcate from the planar Liapunov orbits around the collinear libration points at a given amplitude (see [3], [4], [10], [11], [25]). At the bifurcation, due to the symmetry of the equations of motion, two families of halo orbits appear. These two families are symmetric with respect to the (x, y) plane and, according to [21], are called families of halo orbits of class I and II. Each one is an uniparametric family of orbits which can be parametrized by the z-amplitude (at least locally). For small z-amplitudes the period of the halo orbits is, roughly, one half of the period of the primaries.

Richardson [20] introduced, for the RTBP, reference systems and a formulation suitable for the study of the motion around the collinear libration points. Both are specially useful for the analytical computation of halo orbits by means of the Lindstedt-Poincaré procedure. With the help of ad hoc algebraic manipulators, halo orbits can be computed in a fast way by this procedure up to a high order, which give very accurate solutions (see [5], [6]).

Extending the RTBP to the real solar system, taking for instance the Sun and the Earth-Moon barycentre as primaries, halo orbits are no longer periodic but quasiperiodic (see [1], [16], [17]). This is due to the fact that the perturbations of the bodies of the solar system act in a quasiperiodic way, at least for a moderate time span of a few centuries. For this new vector field and a given time interval, quasiperiodic halo orbits can also be computed accurately ([5], [6]).

The methodology developed in this paper can be applied to any family of halo orbits around any collinear equilibrium point of a RTBP (i.e.: Sun–Jupiter, Sun–Mars, Earth–Moon, Earth–Sun,...). In this paper we present the computations done for the Sun-Earth+Moon system around the libration point L_1. This point is located between the two primaries at approximately 1 500 000 km from the Earth. Halo type orbits around this point give suitable sites to locate artificial satellites devoted to the study of the Sun. They were already used in 1978 by the NASA mission ISEE-3. The SOHO spacecraft, launched in 1996, is using this kind of solution as a nominal orbit too (see [3], [4], [5], [6], [7], [8], [9], [12], [15], [22], [23]).

Halo orbits located around the equilibrium point, L_2, behind the small primary in the Sun-Earth+Moon system (also at roughly 1 500 000 km from the Earth) are of interest in the study of the geomagnetospheric tail at large geocentric distances and the cosmic background radiation (Primordial Structures Investigation (PSI) mission). The same kind of orbits, but in the Earth-Moon system, can be useful for the communications with a translunar base.

In this paper we develop a method for performing the transfer between halo orbits around the same equilibrium point. To solve efficiently this problem gives a greater flexibility in trajectory design and offers more options to a mission.

Our interest on this problem was initially motivated by the study of the transfer from the vicinity of the Earth to a halo orbit around the equilibrium point L_1 of the Earth-Sun system ([6], [7], [19]). There, it was shown that the invariant stable manifolds of halo orbits can be used efficiently for the transfer from the Earth, if we are able to inject the spacecraft into that manifolds. This can be achieved easily when the orbits of the manifold come close to the Earth. But this is true only when the halo orbit is large enough, or when the effect of the Moon, bending some orbits of the manifold, is big enough to take these orbits near the Earth. For small halo orbits, if a swingby with the Moon is used, there are launch possibilities only during two or three days per month ([2], [7], [9], [19]). These launching possibilities can be longer for halo orbits with larger z-amplitude. This is because they have a stable manifold coming closer to the Earth. After the transfer from the Earth to a large halo orbit has been done, we must be able to go from it to a smaller one in a not very expensive way, in terms of the Δv consumption and time.

The methods that we present are based on the local study of the motion around the halo orbits and make use of the geometry of the problem in the neighbourhood of an orbit of this kind [19]. They are completely different from the procedure developed by Hiday and Howell [13], [14]. In their approach they select a departure and arrival states on two arbitrary halo orbits, and take as a path connecting these states a portion of a Lissajous trajectory. At the patch points there are discontinuities in the velocity which must be minimized. The primer vector theory (developed by Lawden [18] for the two body problem) is extended to the RTBP and applied to establish the optimal transfers.

Looking at the cost of the transfers, the first method of Hiday and Howell [13] needs about 120 m/s for going from an initial halo orbit with z-amplitude of 110 000 km to a final one of 240 000 km. These results are improved in the second paper [14] and are close to the ones that we obtain. The cost of this transfer is about 70 m/s. Moreover, it has been observed that the cost of the transfer is almost a linear function of the difference between the z-amplitudes of the initial and final orbits, specially for small z-amplitudes. A comparison of the Hiday–Howell results with the ones obtained in the present paper is given at the end of Section 7.

In a first approach, and to present the key ideas in a simple way, we consider as a model of motion for the spacecraft the spatial restricted three body problem, with the Sun as the big primary located on the positive x-axis and the Earth+Moon barycentre as the small primary lying on the same axis on the negative side. The value of the RTBP mass parameter that has been used in the computations is the one obtained using the values of the masses of the Sun, Earth and Moon given by the JPL ephemeris. These ephemeris will be used for the study of the problem in the real situation, including all the main bodies of the solar system.

The paper begins with the introduction of the geometrically relevant magnitudes for our purposes. Then a first approach is presented to solve the problem, based in some "heuristic" considerations. Numerical results and optimization are included. A second method, based on a detailed analysis of the linear case, is then presented and further examples are given. The method allows to understand the characteristic features of the first approach. Finally, the method is extended when the full solar system is taken into account. A final discussion, conclusions and outlook end the paper.

For reference, we collect here some basic numerical data and definitions used in this work, where *Barycentre* denotes the Earth–Moon barycentre.

$$
\begin{array}{lcl}
\text{Mass parameter} = \mu & = & \dfrac{\text{Mass of Barycentre}}{\text{Mass of Barycentre + Sun}} = 3.04018792067404 \times 10^{-6}. \\
\text{Adimensional unit of distance} & = & \text{Barycentre} - \text{Sun distance} = 1.49597905818 \times 10^{8} \text{ km}. \\
\text{Adimensional unit of velocity} & = & \text{Barycentre velocity with respect to the Sun} \\
 & = & 29784.7358 \text{ m/s}. \\
\text{Adimensional unit of time} & = & \frac{1}{2\pi} \text{ years}. \\
\text{Normalized unit of distance} & = & \text{Barycentre} - L_1 \text{ distance} = 1.497610387 \times 10^{6} \text{ km}. \\
z\text{-amplitude} & = & \text{amplitude of the first Fourier harmonic of} \\
 & & \text{the } z \text{ component of the halo orbit, in km}. \\
\text{Normalized } z\text{-amplitude} = \beta & = & \dfrac{z\text{–amplitude}}{\text{normalized unit of distance}}.
\end{array}
$$

2 Geometric Magnitudes Related to the Halo Orbits

The understanding of the geometry and behaviour of the orbits near a halo one is a key point in the development of good station keeping strategies (see [5], [6]) and it has been shown to be useful also in the problem under consideration.

Consider the equations of the RTBP written as a first order differential system in the following compact form

$$\dot{y} = f(y), \quad y \in \mathbb{R}^6.$$

The study of the neighbourhood of a halo orbit can be done by means of the first order variational equations

$$\dot{A} = Df(y(t))A,$$

with $A(0) = Id$ and $A \in \mathcal{L}(\mathbb{R}^6, \mathbb{R}^6)$.

Denoting by ϕ the flow associated with the differential equations of motion, and by $\phi_\tau(y)$ the image of a point $y \in \mathbb{R}^6$ at $t = \tau$, for $h \in \mathbb{R}^6$ we have

$$\phi_\tau(y+h) = \phi_\tau(y) + D\phi_\tau(y)h + O(\mid h \mid^2) = \phi_\tau(y) + A(\tau)h + O(\mid h \mid^2).$$

For a periodic orbit of period T, the variational matrix after one period, $A(T)$, is called the monodromy matrix associated with the orbit. For small and medium size halo orbits, the analysis of the eigenvalues of the monodromy matrix, $\lambda_1, \ldots, \lambda_6$, shows that

$$\lambda_1 > 1,\ \lambda_2 < 1,\ \lambda_3 = \lambda_4 = 1 \ \text{ and } \ \lambda_5 = \bar{\lambda}_6 \text{ complex with modulus } 1.$$

These six eigenvalues can be gathered by pairs with the following geometrical meanings

- The first two real ones, (λ_1, λ_2), verify $\lambda_1 \cdot \lambda_2 = 1$, and are related to the hyperbolic character of the orbit. λ_1 is the largest one in absolute value, and its related eigenvector, which we shall denote by $e_1(0)$, gives the most expansive direction. Using $D\phi_\tau$ we can get the image of this vector under the variational flow

  $$e_1(\tau) = D\phi_\tau e_1(0).$$

  $e_1(\tau)$ together with the vector tangent to the orbit give, at each point of the orbit, the tangent plane to the local unstable manifold W^u_{loc}.

  In the same way λ_2 and its related eigenvector, $e_2(0)$, are related to the stable manifold and

  $$e_2(\tau) = D\phi_\tau e_2(0),$$

together with the vector tangent to the orbit, give the tangent plane to the local stable manifold, W^s_{loc}, at each point.

Moreover, due to a symmetry in the equations of the RTBP, if $(v_1, \ldots, v_6)$ is the eigenvector associated with λ_1, then $(v_1, -v_2, v_3, -v_4, v_5, -v_6)$ is the one associated with λ_2.

Numerical computations show that halo orbits are very unstable, and that the unstability decreases as the z-amplitude increases. In this way, for a halo orbit of $\beta = 0.08$ ($z_{\max}$ ≈120 000 km) we have $\lambda_1 \simeq 1727.96$ while for $\beta = 0.25$, ($z_{\max}$ ≈375 000 km) $\lambda_1 \simeq 1420.67$.

- The second couple (λ_3, λ_4), has both eigenvalues equal to 1 and they are related to neutral directions (i.e., non-unstable modes). But in spite of the fact that 1, as eigenvalue, has algebraic multiplicity equal to two, its geometric multiplicity is only one. So, there is only one eigenvector of $A(T)$ with eigenvalue equal to 1. It is the vector tangent to the orbit, which will be denoted by $e_3(\tau)$.

  The other eigenvalue is related to variations of energy or of any variable which parametrizes the family of halo orbits within our range of small and medium size orbits, for instance the z-amplitude. The related vector, which is chosen orthogonal to $e_3(0)$ in the 2-dimensional space associated with the eigenvalue 1, gives the tangent direction to the family of halo orbits. The monodromy matrix restricted to this plane has the Jordan form

$$\begin{pmatrix} 1 & \varepsilon \\ 0 & 1 \end{pmatrix}.$$

  The fact that ε is not zero, is because the period of the halo orbits changes (it decreases very slowly when β increases) along the family.

- The third couple (λ_5, λ_6) is composed by two conjugated complex eigenvalues of modulus 1. Together with the previous couple they complete the part associated with the central manifold of the orbit. The monodromy matrix restricted to the plane generated by the real and imaginary parts of the eigenvectors related to λ_5 and λ_6 is a rotation, so it has the form

$$\begin{pmatrix} \cos\Gamma & -\sin\Gamma \\ \sin\Gamma & \cos\Gamma \end{pmatrix}.$$

Summarizing the above results we can state that, in a suitable basis, the monodromy matrix associated with a halo orbit can be written in the form

$$\left(\begin{array}{cc|cc|cc} \lambda_1 & & & & & \\ & \lambda_1^{-1} & & & 0 & \\ \hline & & 1 & \varepsilon & & \\ & & 0 & 1 & & \\ \hline & 0 & & & \cos\Gamma & -\sin\Gamma \\ & & & & \sin\Gamma & \cos\Gamma \end{array}\right).$$

Instead of the vectors $e_i(\tau)$, $i = 1,\ldots,6$, it is more convenient to introduce the *Floquet modes*, $\bar{e}_i(\tau)$, $i = 1,\ldots,6$, as six T-periodic functions, where T is the period of the halo orbit. From them the vectors $e_i(\tau)$ are easily recovered [24]. This is done because periodic functions can be spanned in Fourier series and easily stored by means of its Fourier coefficients.

We define the first Floquet mode taking into account that the rate of escape from the halo orbit along the unstable manifold is exponential

$$\bar{e}_1(\tau) = e_1(\tau)\exp\left(-\frac{\tau}{T}\ln\lambda_1\right).$$

The second one is defined in an analogous way taking into account that the rate of approximation along the stable manifold is also exponential

$$\bar{e}_2(\tau) = e_2(\tau) \exp\left(-\frac{\tau}{T} \ln \lambda_2\right).$$

The third one is the vector tangent to the halo orbit. As it is already a periodic function we simply put

$$\bar{e}_3(\tau) = e_3(\tau).$$

For the fourth one we split $e_4(t)$ as

$$e_4(\tau) = \bar{e}_4(\tau) + \varepsilon(\tau)\bar{e}_3(\tau),$$

where $\bar{e}_4(\tau)$ is chosen orthogonal to $\bar{e}_3(\tau)$ in the plane spanned by $e_3(\tau)$ and $e_4(\tau)$.

Finally the fifth and sixth modes are computed taking into account that as we have said, the monodromy matrix restricted to the plane generated by the real and imaginary parts of the eigenvectors associated with λ_5 and λ_6 is a rotation, so we define

$$\begin{aligned}
\bar{e}_5(\tau) &= \cos\left(-\frac{\Gamma\tau}{T}\right) e_5(\tau) - \sin\left(-\frac{\Gamma\tau}{T}\right) e_6(\tau), \\
\bar{e}_6(\tau) &= \sin\left(-\frac{\Gamma\tau}{T}\right) e_5(\tau) + \cos\left(-\frac{\Gamma\tau}{T}\right) e_6(\tau),
\end{aligned}$$

where Γ is the angle of rotation. Γ is the argument of $\lambda_5 = a + bi$ as a complex number. Note that it is only defined modulus 2π. Any determination will give T-periodic vectors $\bar{e}_5$ and $\bar{e}_6$. But it is convenient to take the determination which produces the highest constant terms in the Fourier expansion of $\bar{e}_5$ and $\bar{e}_6$.

For further use we introduce now the *projection factors*. Assume that at a given epoch, τ, the state (in the phase space of positions and velocities) of a spacecraft is given by $S \in \mathbb{R}^6$ and it is close to a certain halo orbit. We associate to the point S another one on the halo orbit, $N \in \mathbb{R}^6$, which will be called the *nominal point* of S. Different nominal positions can be defined according to different criteria. Some particular ones will be introduced in Section 3.

The difference

$$\delta = S - N = (\delta x, \delta y, \delta z, \delta \dot{x}, \delta \dot{y}, \delta \dot{z}),$$

can be expressed as a linear combination of the Floquet modes

$$\delta = \sum_{i=1}^{6} c_i \bar{e}_i(\tau).$$

By using elementary linear algebra we have that

$$c_i = \pi_1^i(\tau)\delta x + \pi_2^i(\tau)\delta y + \pi_3^i(\tau)\delta z + \pi_4^i(\tau)\delta \dot{x} + \pi_5^i(\tau)\delta \dot{y} + \pi_6^i(\tau)\delta \dot{z},$$

where, given the Floquet matrix $(\bar{e}_1(\tau), ..., \bar{e}_6(\tau))$, the value of $\pi_j^i(\tau)$ is equal to the adjoint of the j-th element of the i-th column, divided by the determinant of the matrix.

We see that we can compute the c_i component doing the scalar product of the error vector δ and $\pi^i = (\pi_1^i, ..., \pi_6^i)$ which is called the i-th *projection factor*. It is clear that the projection factors depend only on $\bar{e}_i(\tau)$. In practice it is convenient to compute them at the same time that we compute the Floquet modes and store them by its Fourier coefficients, in the same way that is done with the Floquet modes.

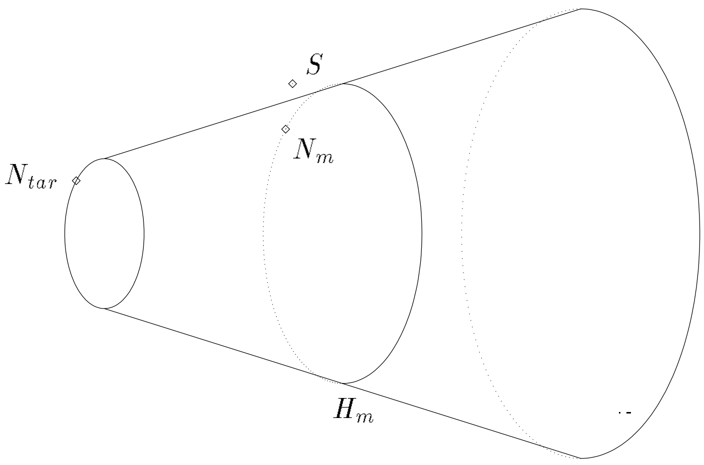

Figure 1: Qualitative representation of the family of halo orbits and some relevant points.

As a technical matter, due to the fact that the norms of $\bar{e}_i(\tau)$ change with the time τ, it is better to perform some normalization multiplying π^i by $\|\bar{e}_i\|$. In this way the c_i are always given with respect to vectors of modulus one. That is, if we write

$$\delta = \sum_{i=1}^{6} c_i \frac{\bar{e}_i(\tau)}{\|\bar{e}_i(\tau)\|},$$

we get $c_i = \|\bar{e}_i\| < \pi^i, \delta >$, where $< \ , \ >$ denotes the scalar product.

3 A First Approximation to the Transfer

The goal of this Section is to define a strategy to perform the transfer between halo orbits. To clarify it, we use a qualitative representation of the family of halo orbits, in the configuration space, as a piece of a cone. On it, each halo orbit is identified as a circle and its radius can be seen as the z-amplitude. With this representation the problem is to go from one circle to another one by making use of the dynamics near the cone described in the preceding Section.

Assume that the spacecraft is at a certain point, $S = (S^p, S^v)$ of the phase space. S^p stands for positions and S^v for velocities. In general S will not be on the family of halo orbits but close to it. We denote by $N_m = (N_m^p, N_m^v)$ the closest point in the family taking into account only their spatial coordinates (with $||N_m^p - S^p||$ minimum). We call N_m the *nominal point of* S *at minimum distance* and we denote by H_m the halo orbit which contains N_m. H_m is the *nominal orbit at minimum distance* (see figure 1 for the representation in the configuration space). To the point N_m we can associate an angle α_m on the orbit H_m.

It seems natural that if we want to move along the family of halo orbits we must do a manoeuvre in the direction tangent to the family of orbits. There seems to be two natural ways of performing this with, in principle, no clear advantages of any of them in front of the other.

1. The first one considers the vector going from a point, N_{tar}, chosen in a target halo orbit, H_{tar}, and with the same angle, α_m, to the actual position of the spacecraft, S. The manoeuvre is performed in such a way that the tangent to the family component of this vector is cancelled. This manoeuvre produces some kind of libration between the initial and the target halo orbits as it will be clear later on.

2. The second procedure, which keeps the same libration features, performs the tangent to the family impulse (that is Δv has components proportional to the velocity components of the tangent to the family vector) in such a way that the vector from the nominal point at minimum distance, N_m, to the spacecraft, S, (a vector that is zero if S is on a halo orbit) has only tangent to the family, tangent to the orbit and the two neutral components. The tangent impulse adds to the natural libration around a halo orbit an additional one along the family of halo orbits.

For the first procedure, that will be used in Sections 4 and 5, we compute *unitary controls* $(\Delta_1, \Delta_2, \Delta_3)$, along the x, y, and z directions respectively. We define them in order to cancel the unitary tangent to the family component, in such a way that when we add both, the resulting vector has only stable, $\bar{e}_2$, tangent to the orbit, $\bar{e}_3$, and the two neutral components, $\bar{e}_5$, $\bar{e}_6$. In this way we have,

$$\frac{\bar{e}_4(\tau)}{\|\bar{e}_4(\tau)\|} + \begin{pmatrix} 0 \\ 0 \\ 0 \\ \Delta_1 \\ \Delta_2 \\ \Delta_3 \end{pmatrix} = \alpha_2\bar{e}_2(\tau) + \alpha_3\bar{e}_3(\tau) + \alpha_5\bar{e}_5(\tau) + \alpha_6\bar{e}_6(\tau).$$

The different vectors $\bar{e}_j(\tau)$, $j = 2, ..., 6$, should be computed taking H_{tar} as basic orbit.

If one considers that the initial and final values of β, that is, the z-amplitudes of the orbits H_m and H_{tar}, are close, one can do an approximation by using the $\bar{e}_j$ vectors at the point N_m of the H_m orbit. As the Floquet modes, $\bar{e}_i(\tau)$ are known, from the first three equations, the coefficients α_2, α_5 and α_6 are obtained as a function of α_3. Inserting these results in the last three equations we get Δ_1, Δ_2 and Δ_3 as a function of α_3. Adding some optimal condition such as

$$\|\Delta\|_2 = (\Delta_1^2 + \Delta_2^2 + \Delta_3^2)^{1/2},$$

to be a minimum, the value of α_3 is then fixed and Δ_1, Δ_2 and Δ_3 can be computed and stored for any point of a halo orbit. According to the thrusters used and to the kind of stabilization of the spacecraft, other norms, such as:

$$\|\Delta\| = | \Delta_1 | + | \Delta_2 | + | \Delta_3 | \quad \text{or} \quad \|\Delta\| = (\Delta_1^2 + \Delta_2^2)^{1/2} + | \Delta_3 |,$$

can be more adequate. This amounts to elementary modifications of the algorithm.

For an efficient implementation of the transfer between two halo orbits, a mesh of orbits must be precomputed. For them the unitary controls, Δ_i, are stored using its Fourier series. Then, for any orbit of the family, its unitary controls, at a given epoch t, are obtained by interpolation. Tangent impulses are computed multiplying the projection on the direction tangent to the family by the unitary controls. This is the procedure used in the numerical explorations, described in the next Section, for the RTBP.

For the second method, that is used in Section 8, we perform a manoeuvre Δv_T such that,

$$\begin{pmatrix} S^p \\ S^v + \Delta v_T \end{pmatrix} - \begin{pmatrix} N_m^p \\ N_m^v \end{pmatrix} = \alpha_3\bar{e}_3(\tau) + \alpha_4\bar{e}_4(\tau) + \alpha_5\bar{e}_5(\tau) + \alpha_6\bar{e}_6(\tau).$$

The vectors $\bar{e}_j(\tau)$, $j = 3, ..., 6$, are computed taking H_m as basic orbit. The vector Δv_T has components proportional to the velocity components of the tangent to the family vector $\bar{e}_4(\tau)$.

As before we have one degree of freedom for choosing the components of Δv_T. It has been fixed by choosing the magnitude of the manoeuvre, $\|\Delta v_T\|$, since other procedures such that maximize the tangent to the family component with respect to the cost of the manoeuvre do not give clear advantages.

In addition to the *tangent to the family manoeuvre* (from now on **TFM**) at the departure orbit, an *insertion manoeuvre* (from now on **IM**) into the target halo orbit must be done to complete the transfer. Together they constitute a *jump manoeuvre* (from now on **JM**).

Given a point S in the phase space, close enough to the family of halo orbits, we attach to it a nominal point, N_w, which will be on a halo orbit H_w. This point is chosen in such a way that when performing a suitable manoeuvre the spacecraft is injected into the stable manifold of the halo orbit H_w. For this purpose the only thing we need is that the error vector, $\delta_w = S - N_w$, verifies

$$(\delta_w)_i = \lambda \cdot (\bar{e}_2)_i, \quad i = 1, 2, 3,$$

for some real λ. This is, we look for N_w such that $\bar{e}_2$ and δ_w are parallel in the space of positions. Then, if we modify the velocity of the spacecraft by adding the last three components of $\lambda \cdot \bar{e}_2 - \lambda_w$, we have that the new error vector, δ_w, will be a multiple of $\bar{e}_2$, (and so, in the linear approximation of the stable manifold of H_w). In this way, after doing the IM, the satellite will go asymptotically to H_w.

4 Computation of Tangent to the Family Manoeuvres and some numerical results

In this Section we show how we perform a TFM and the evolution of the trajectory after it.

Due to the periodic character of halo orbits, they can be trivially parametrized by an angle $\alpha \in [0, 360]$. So, a point on the family of halo orbits is identified by an angle and a z-amplitude (this has been very useful in the practical implementation). In our computations the origin of the angles is at $y = 0$, $z > 0$ (and, hence, $\dot{x} = \dot{z} = 0$), increasing in the sense of the orbit.

Numerical explorations show that unitary controls Δ_i, and so the value of $\|\Delta\|$, depend strongly on the angle, α, at which the TFM is done. Moreover, a TFM towards a selected orbit does not imply that we tend asymptotically to it.

It seems natural to classify TFM by its magnitude. Given a certain state S of the spacecraft and an amount of Δv, we look for the manoeuvre to be done in order to do a TFM of the required magnitude. The procedure is to look for a point on a halo orbit such that its tangent to the family component is cancelled by the manoeuvre. During the search of this point, the z-amplitude is varied whilst the angle is kept equal to the one of the nominal point at minimum distance, N_m, of S. In this way we can perform TFM of the same magnitude from different angles of a selected halo orbit and to compare them.

Figure 2 shows the evolution of the z-amplitude of the nominal orbits at minimum distance of three trajectories in front of the elapsed time. The trajectories are obtained by doing TFM of 10 m/s, 1 m/s and 10 cm/s at 0° on a halo orbit of z-amplitude 0.15 (225 000 km approximately). All the integrations have been carried out during a time span equal to the period of the initial halo orbit (roughly, 6 months).

From this figure it can be seen that after a complete revolution there is not a significant decrease of the z-amplitude. Only near 0.8 and 2.3 units of adimensional time (approx. 46 and 133 days respectively) a large decrease of the z-amplitude takes place, if the TFM is large enough, but this decreasing is not preserved during a full revolution. In a certain way we escape through the tangent direction but keeping the libration. As the TFM is done in the center-stable manifold what we get is another type of libration.

In the qualitative representation of the family of halo orbits, the orbit obtained with the TFM should be seen as in figure 3.

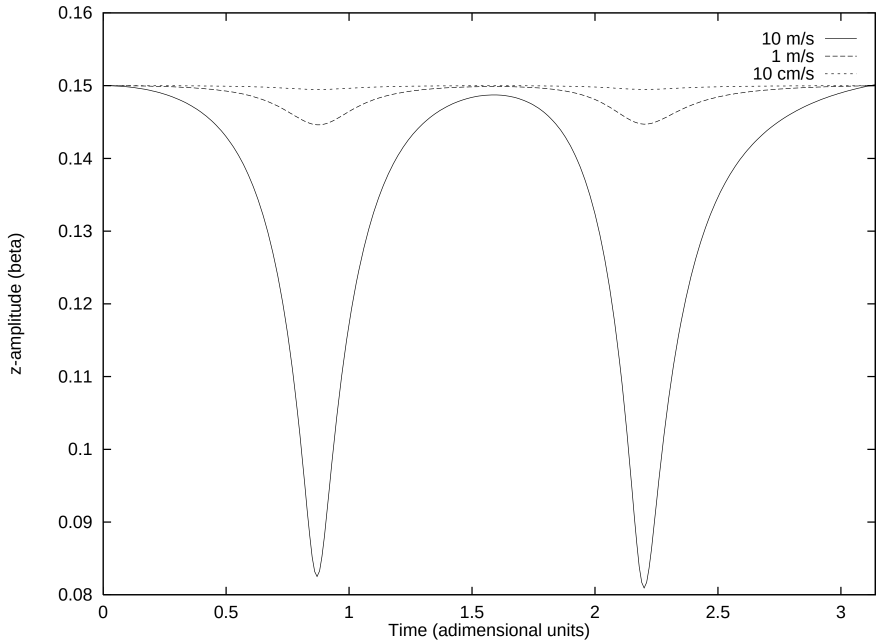

Figure 2: Evolution of the z-amplitude vs time when a TFM is done. The three curves correspond, respectively, to TFM done at $\alpha = 0$ and of magnitude 10 m/s, 1 m/s and 10 cm/s, on a halo orbit with z-amplitude $\beta = 0.15$. On the horizontal axis adimensional time is represented for a time span covering one period of the orbit. On the vertical axis the normalized z-amplitude, β, of the halo orbit, H_m, at minimum distance of the moving point is given.

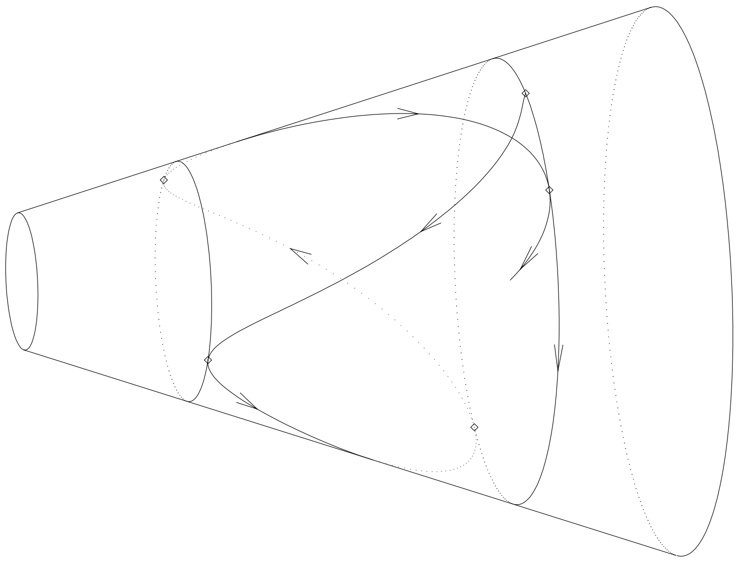

Figure 3: Qualitative representation of the evolution of a trajectory, projected on the family of halo orbits by means of the N_m point, when a TFM is done to decrease its z-amplitude.

For a fixed Δv, numerical explorations of transfer trajectories starting from different angles, α, show the following behaviour:

1. Qualitatively, the evolution of the z-amplitude is always the same. It varies in a regular way, between two extreme values, the initial one and some final one depending on α.

2. Depending on the value of α, the concavity of the z-amplitude curve shown in figure 2 between its extrema, changes too. Concavities as the one in figure 2 give better performance in the sense that lower z-amplitudes are reached.

3. The behaviour is completely similar when the transfer is done in the sense of increasing z-amplitudes.

In Section 3 two different procedures were described. It was stated that no one of them has clear advantages over the other. To put this in evidence the following computation has been done. Assume that the spacecraft is exactly located on the H_m orbit. By definition, the TFM using the second procedure has components proportional to the velocity components of $\bar{e}_4$. The first method proceeds in a slightly different way. But, if we consider the typical "best" place to do the first manoeuvre, that is, with $\alpha = 0$, the angle of the two possible Δv, using one method or the other, is very close to 18^o, for the full range of interesting values of β. Hence, the two procedures are rather close.

5 Optimization of the Jump Manoeuvre

The previous results suggest that, in order to go from one halo orbit to another one, one can try two different manoeuvres: the TFM one at departure and, some time later, an IM. Both manoeuvres considered together define a *jump manoeuvre*, JM.

In order to optimize a JM, we note that it depends on three parameters:

1. The epoch at which the TFM is done, t_T, or equivalently, due to the fact that the restricted three body problem is autonomous, the angle in the initial halo orbit where the satellite is located, α_T.

2. The magnitude of the TFM, Δv_T.

3. The epoch at which the IM is performed, $t_I = t_T + \Delta t$. We note that, given t_T and Δv_T, the magnitude of the IM, Δv_I, depends only on t_I.

We define the *performance of the jump manoeuvre* as

$$P_J = \frac{\Delta\beta}{\Delta v_T + \Delta v_I},$$

where $\Delta\beta$ is the difference between the amplitude of the halo orbit at which we do the TFM and the amplitude of the halo orbit, H_w, at which we tend when we perform the IM.

In a first step, we have done a numerical study of the function P_J, keeping the initial point (α_T) fixed, doing some TFM and varying the epoch at which the IM is performed. These explorations have been done for different values of the TFM. The results show that for a fixed initial α_T, the optimum epoch of insertion, t_I, is almost independent of the magnitude of the TFM. This is shown in figure 4 where the function P_J is plotted in front of the insertion epoch t_I, for TFM of 5 m/s (dotted line) and 10 m/s (solid line), both given at $\alpha_T = 0^o$ on an initial halo orbit of z-amplitude $\beta = 0.20$.

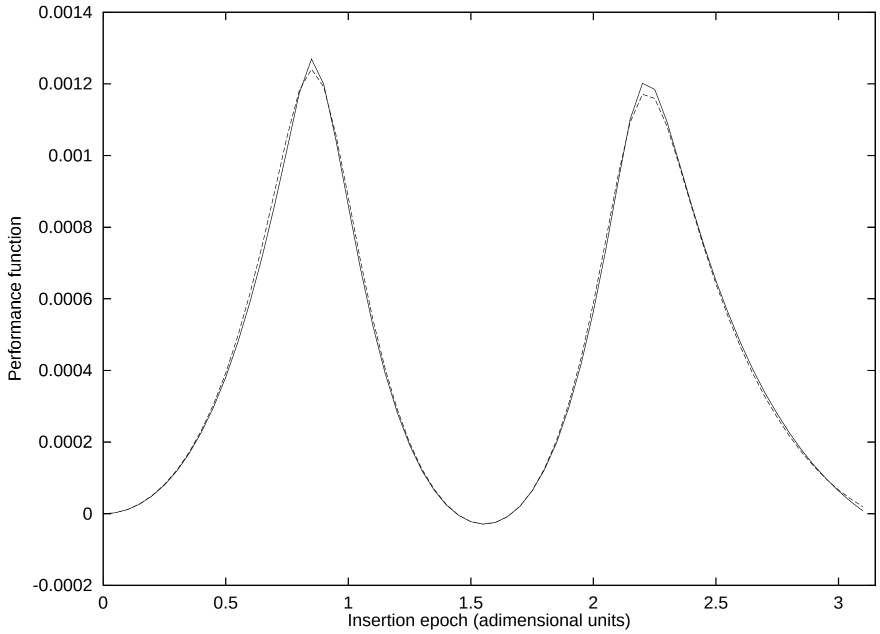

Figure 4: Performance function, P_J, (measured in $\Delta\beta\ m^{-1}s$) in front of the insertion epoch t_I (in adimensional units). The function is plotted for two different values of Δv_T. The solid line corresponds to a TFM of 10 m/s and the dotted one to 5 m/s. The time span covers one period of the halo orbit. The initial halo orbit has taken with $\beta = 0.20$.

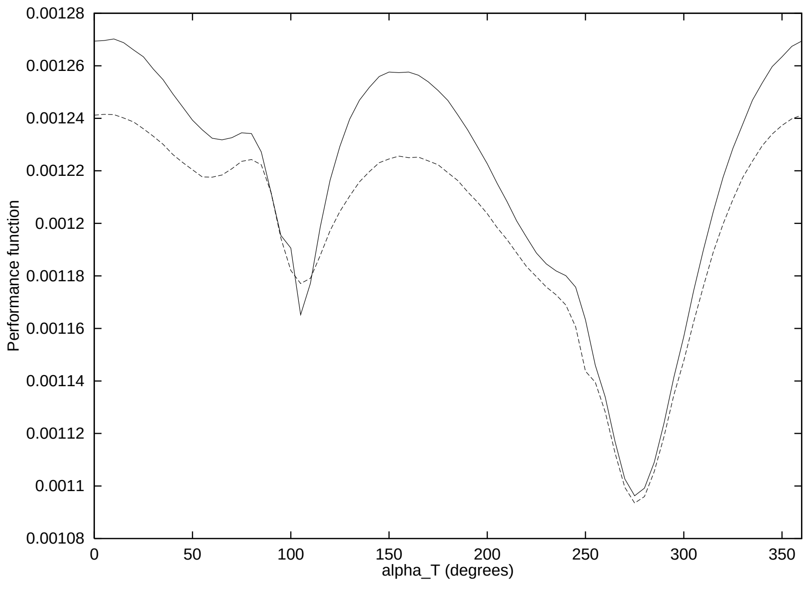

Figure 5: Performance function, P_J, (in $\Delta\beta\ m^{-1}s$) in front of the angle α_T (in degrees). For each α_T, the IM is done at its corresponding optimum epoch. The solid line corresponds to a TFM of 10 m/s and the dotted one to 5 m/s. The initial halo orbit has taken with $\beta = 0.20$.

Once we know that the optimum insertion epoch, t_I, looks like independent of the magnitude of the TFM (at least for moderate values of Δv_T), and depends only on α_T, we study the function

$$P_J(\Delta v_T, \alpha_T, t_I(\alpha_T))$$

when the angle α_T varies, and for different values of Δv_T. The result is given in figure 5 for values of TFM equal to 10 m/s (solid line) and to 5 m/s (dotted line).

From the last figure we see that for a TFM of 10 m/s given at $\alpha_T = 0^o$, the performance of the method is of $1/1.27 \times 10^{-3}$= 787.40 $\Delta v/\Delta\beta$ (Δv in m/s). Hence the cost for going from a halo orbit of normalized z-amplitude $\beta = 0.25$ to one with $\beta = 0.08$ must be of 133.86 m/s (assuming perfect linearity, of course). As it is clear from figure 4, if we do the TFM at $\alpha_T = 0^o$, the IM must be done after 0.8 units of RTBP time which is, roughly, 46 days.

It is worth to note from figure 5, that a similar performance is obtained for values of α_T close to 180^0, whilst the worst situations correspond near 100^o and 270^o.

Figure 6 shows the projections on the coordinate planes of a transfer trajectory that goes from a halo orbit of amplitude $\beta = 0.25$ to another one with $\beta = 0.08$. For the whole transfer three JM have been done, all of them with the same size of the TFM, and equal to 15.57 m/s. The total Δv is 148.6 m/s. This is slightly larger than predicted before, because linearity was assumed and no optimization has been done about how to split the different JM and the epochs to do the last two TFM.

Figure 6 must be seen together with figure 7 where the evolution of β versus time is plotted. The two amplitudes represented correspond to the nominal orbits H_m (solid line) and H_w (dotted line). This is only an example to illustrate the method, but we insist in that the manoeuvres have not been performed in the optimum way. That is, for each jump, TFM are not always done at the optimal places, but IM are always performed in the optimal way to maximize the performance of that jump with the fixed value of α_T.

We explain these three JM with some detail:

1. The first TFM is done when $t = 0$ at $\alpha_T = 0^o$, and the IM of 51.27 m/s is performed after 0.8 units of time (for a value of the angle α close to 90^o). This JM decreases the z-amplitude of the halo orbit from 0.25 to 0.17 approximately.

2. The second TFM has been done at t near 2.3 units of time, for a value of α close to 270^o. We note (from figure 5) that this value of α corresponds to a non optimal one for the performance function. From a practical point of view this is clear since the decreasing of the z-amplitude is smaller than the obtained in the former JM with the same TFM. It is also apparent due to the different behaviour of the concavity of the amplitude function when compared with the former JM. The corresponding IM of 10.25 m/s, which completes the second JM, is done close to $t = 3.1$, near $\alpha = 0^o$.

3. The last TFM has been done approximately at $t = 4.6$ near a value of $\alpha = 180^o$. Again from figure 5 it is seen that this last value is an optimal one, the behaviour being similar to the first JM. The third and final IM of 40.37 m/s is given when $t = 5.3$ at $\alpha = 265^o$.

The total transfer takes approximately 5.5 adimensional units of time, or equivalently, 320 days. This could be too long for a real situation, but due to the fact that keeping fixed the initial angle the optimum time of insertion does not depend on the TFM (figure 4), the transfer can be done with only one JM and lasting a time span equal to the time span of the previous first JM. We will see this in the Section 8 for a more realistic situation.

Figure 8 shows the evolution of the z-amplitude for a transfer between the same orbits of the preceding example, using two optimal JM. Both TFM are of 12.13 m/s and the IM are of 38.16 m/s and 69.12 m/s, which give a total Δv of 131.54 m/s. Figure 9 shows the corresponding

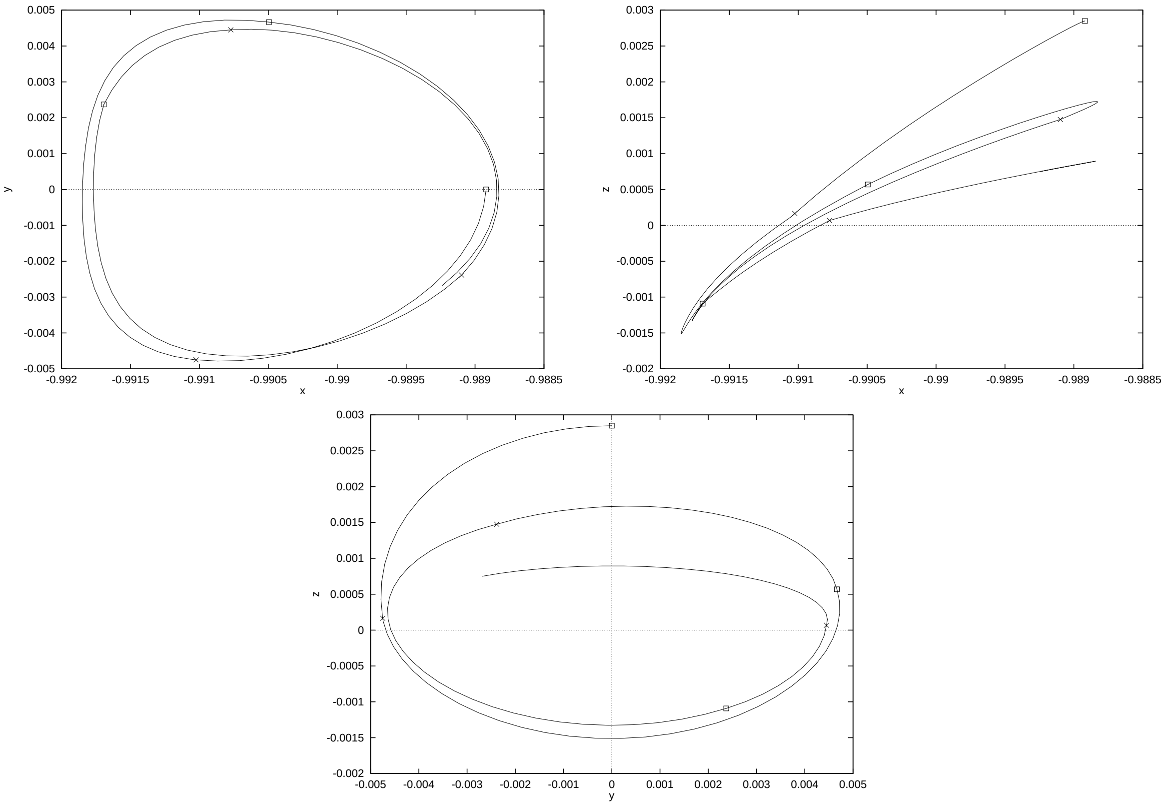

Figure 6: Projections on the coordinate planes of a transfer orbit for the RTBP that goes from a halo orbit of z-amplitude $\beta = 0.25$ to an amplitude $\beta = 0.08$. The units and reference system used for the representation are the adimensional RTBP ones. The points marked with a small box correspond to TFM and those marked with a cross to IM. In this figure, and in all the subsequent figures displaying projections of orbits, the sense of motion in the (x, y) projection is clockwise, while in the (y, z) projection is counterclockwise. The sense in the (x, z) projection can be derived from the other two projections.

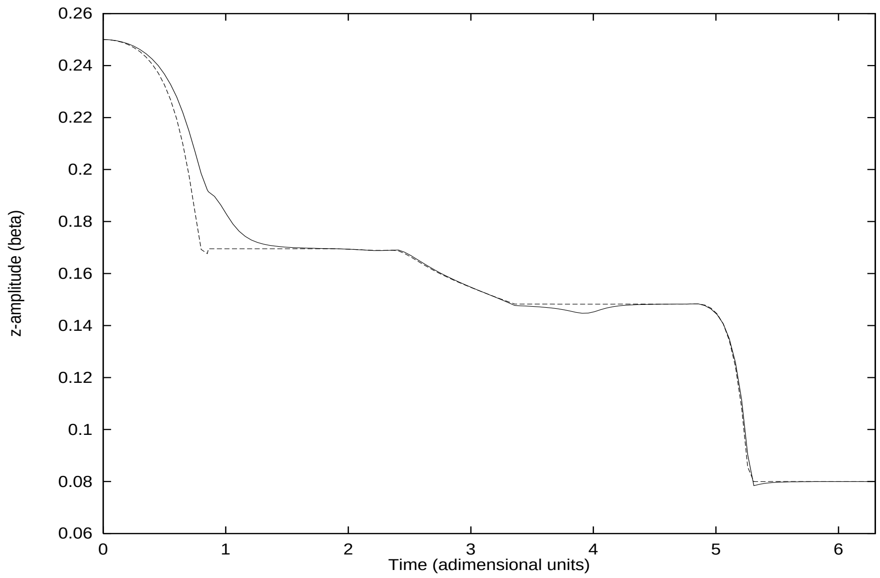

Figure 7: Evolution of the z-amplitude (β) vs time (t), in terms of the nominal orbits H_m (solid line) and H_w (dotted). The transfer corresponds to the orbit plotted in figure 6. Three JM where done with a total Δv expenditure of 148.6 m/s.

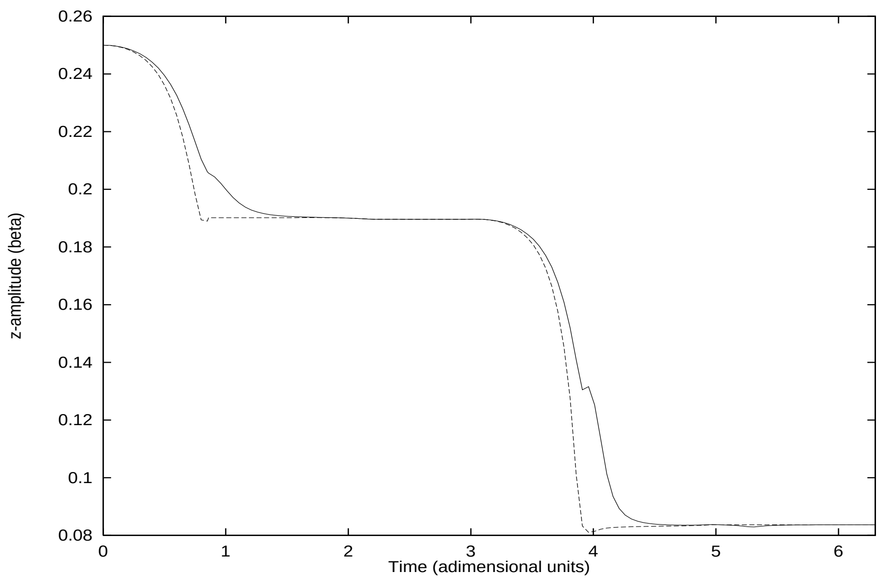

Figure 8: Evolution of the z-amplitude (β) in front of time (t) for a transfer between a halo orbit of z-amplitude $\beta = 0.25$ and a final one of $\beta = 0.08$ for the RTBP. The TFM were done at the optimum values of α_0. The projections of the orbit are plotted in figure 9. Three JM where done with a total Δv expenditure of 131.54 m/s.

projections of the transfer orbit. Figure 10 displays the cumulative Δv used, versus time, for the total JM, both in the non optimal (with 3 JM) and in the optimal (with 2 JM) cases. In both cases the number of jumps can be taken arbitrarily.

6 Linear Approximation of the Problem

In this Section we study the transfer between two halo orbits which are assumed to be very close in the family of halo orbits. With this hypothesis, the linear approximation of the flow in the neighbourhood of the halo orbits, given by the variational equations, is good enough to have a better understanding of the transfer.

Assume that at a given epoch, t_1, we are on a halo orbit, H_1, and that at this point a manoeuvre, $\Delta v^{(1)}$, is performed to go away from the actual orbit. This manoeuvre is, in principle, arbitrary. Hence, it should not be considered as a TFM, as we did before. At $t = t_2 > t_1$, a second manoeuvre, $\Delta v^{(2)}$, is executed in order to get into the stable manifold of a nearby halo orbit H_2. This one is close to an IM, of the type we presented before, but using as approximation of the stable vector, $\bar{e}_2$ the one of the initial halo orbit. Denoting by $\Delta\beta$ the difference between the z-amplitudes of these two orbits, the purpose of an optimal transfer is to perform both manoeuvres in such a way that the performance function

$$\frac{\Delta\beta}{\|\Delta v^{(1)}\|_2 + \|\Delta v^{(2)}\|_2},$$

shall be maximum, as we have explained before.

Let $\beta(0)$ be the initial z-amplitude of a halo orbit. Using the notation introduced in Section 2, the corresponding points in the phase space at $t = t_1, t_2$, and assuming that the time required to execute the manoeuvre can be neglected, will be, respectively,

$$\phi_{t_1}(\beta(0)) + \begin{pmatrix} 0 \\ \Delta v^{(1)} \end{pmatrix}, \quad \text{and} \quad \phi_{t_2}(\beta(0)) + A(t_2)A(t_1)^{-1} \begin{pmatrix} 0 \\ \Delta v^{(1)} \end{pmatrix}.$$

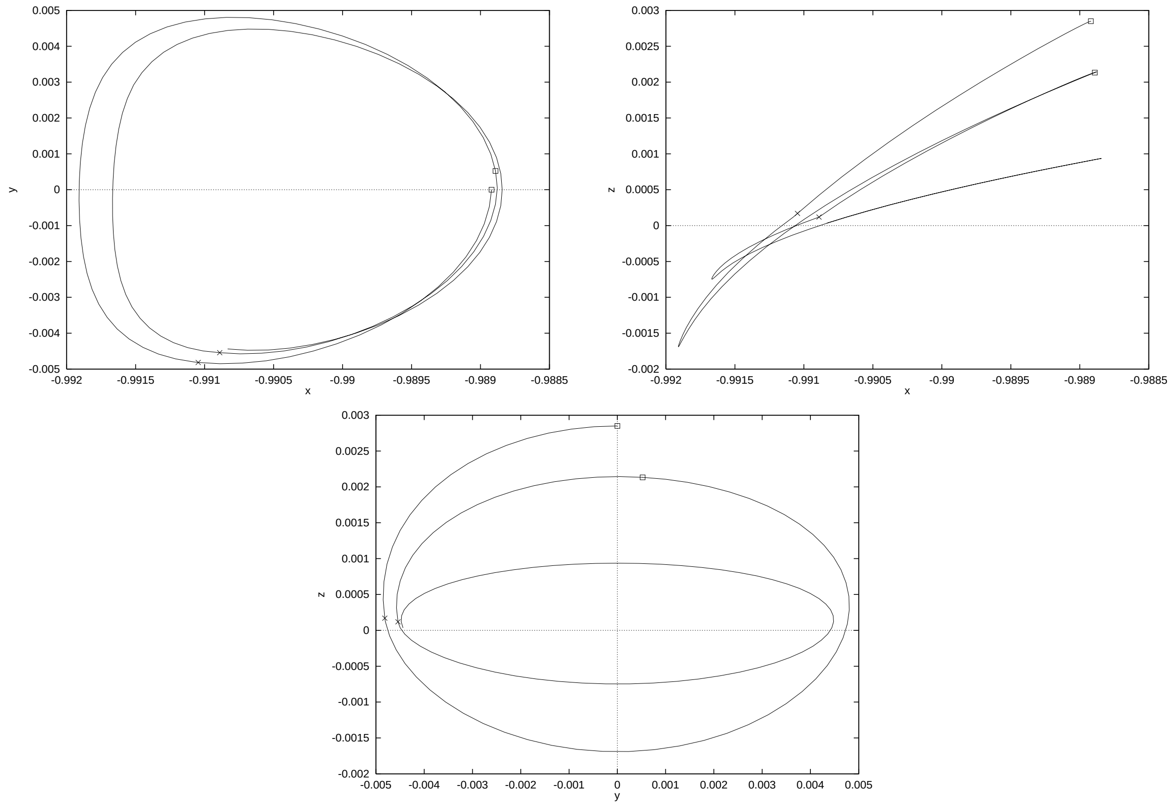

Figure 9: Projections on the coordinate planes of a transfer orbit that goes from a halo orbit of z-amplitude $\beta = 0.25$ to an amplitude $\beta = 0.08$ with optimum TFM. The units and reference system used for the representation are the adimensional ones. The points marked with a small box correspond to TFM and those marked with a cross to IM.

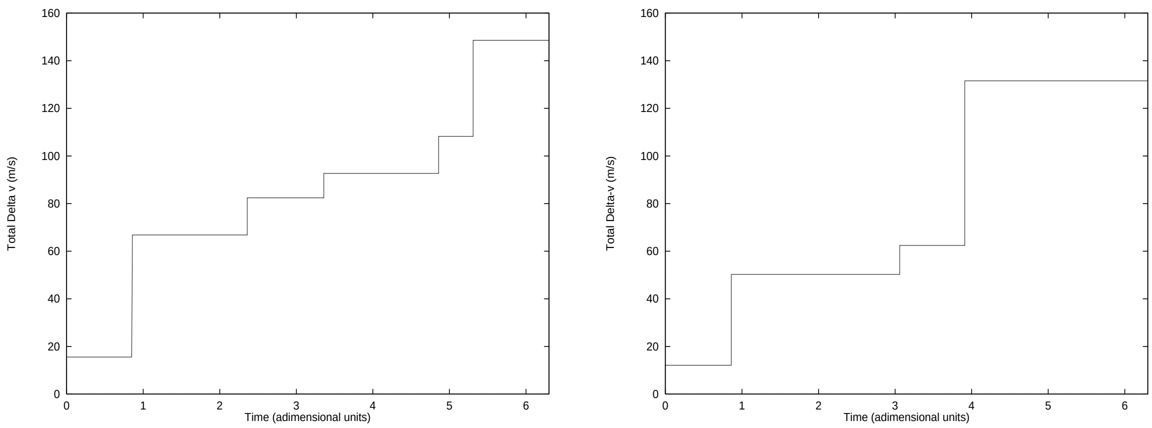

Figure 10: Total Δv (m/s) used vs time (RTBP units). The left plot corresponds to the non optimal transfer and the right one to the optimal transfer.

At $t = t_2$ the IM, $\Delta v^{(2)}$, into the stable manifold of the halo orbit of z-amplitude $\beta + \Delta\beta$ is done. So, we must have

$$\phi_{t_2}(\beta(0)) + A(t_2)A(t_1)^{-1}\begin{pmatrix} 0 \\ \Delta v^{(1)} \end{pmatrix} + \begin{pmatrix} 0 \\ \Delta v^{(2)} \end{pmatrix} =$$

$$= \phi_{t_2}(\beta(0) + \Delta\beta) + \gamma_2 e_{2,\beta+\Delta\beta}(t_2) + \gamma_3 e_{3,\beta+\Delta\beta}(t_2),$$

where $e_{2,\beta+\Delta\beta}(t_2)$ and $e_{3,\beta+\Delta\beta}(t_2)$ are the eigenvectors related to the stable direction and to the tangent to the orbit direction, respectively, of the orbit of amplitude $\beta+\Delta\beta$ at $t = t_2$. The first term in the right hand side of the above equation can be written as

$$\phi_{t_2}(\beta(0) + \Delta\beta) = \phi_{t_2}(\beta(0)) + \frac{\partial\phi_{t_2}(\beta(0))}{\partial\beta}\Delta\beta + O((\Delta\beta)^2).$$

We can also keep only the first order terms of the expansions of e_2 and e_3 in order to write

$$A(t_2)A(t_1)^{-1}\begin{pmatrix} 0 \\ \Delta v^{(1)} \end{pmatrix} + \begin{pmatrix} 0 \\ \Delta v^{(2)} \end{pmatrix}$$

$$= \frac{\partial\phi_{t_2}(\beta(0))}{\partial\beta}\Delta\beta + \gamma_2\left(e_{2,\beta}(t_2) + \frac{\partial e_{2,\beta}(t_2)}{\partial\beta}\Delta\beta\right) + \gamma_3\left(e_{3,\beta}(t_2) + \frac{\partial e_{3,\beta}(t_2)}{\partial\beta}\Delta\beta\right)$$

$$= A(t_2)\frac{\partial\phi_0(\beta(0))}{\partial\beta}\Delta\beta + \gamma_2 A(t_2)\left(e_{2,\beta}(0) + \frac{\partial e_{2,\beta}(0)}{\partial\beta}\Delta\beta\right) + \gamma_3 A(t_2)\left(e_{3,\beta}(0) + \frac{\partial e_{2,\beta}(0)}{\partial\beta}\Delta\beta\right).$$

Note that $e_{2,\beta}(t_2) = A(t_2)e_{2,\beta}(0)$ and $e_{3,\beta}(t_2) = A(t_2)e_{3,\beta}(0)$ are the stable direction vector and the tangent to the orbit vector at $t = t_2$. The partial derivatives of $e_{2,\beta}$ and $e_{3,\beta}$ can be neglected, because γ_2 and γ_3 must be of the order of $\Delta\beta$ and these terms will give a contribution $O((\Delta\beta)^2)$. Hence, the equation above gives $\Delta v^{(1)}$ and $\Delta v^{(2)}$ as linear functions of $\Delta\beta$, γ_2 and γ_3. From now on we normalize by taking $\Delta\beta = 1$.

In principle we could multiply both sides of the above equation by $A(t_2)^{-1}$ to solve for $\Delta v^{(1)}$ and $\Delta v^{(2)}$. This is not good for the numerical computations: if t_2 is close to twice the period of the departure halo orbit, then the components of the transition matrix $A(t_2)$ are of the order of 10^9 and the rounding and truncation errors are amplified through the computations producing not good enough results. Using the autonomous character of the differential equations of the RTBP, it is easy to compute directly the transition matrix $A(t_2)A(t_1)^{-1}$, which, if $t_2 - t_1$ is of the order of magnitude of the period of the orbit, has components of the order of 10^3. The only magnitudes which remain to be computed are $e_{2,\beta}(t_2)$ and $e_{3,\beta}(t_2)$, that can be easily recovered from their corresponding periodic Floquet modes. Denoting by $A_{t_1,t_2} = A(t_2)A(t_1)^{-1}$, we have

$$A_{t_1,t_2}\begin{pmatrix} 0 \\ \Delta v^{(1)} \end{pmatrix} + \begin{pmatrix} 0 \\ \Delta v^{(2)} \end{pmatrix} = \frac{\partial\phi_{t_2}(\beta(0))}{\partial\beta} + \gamma_2 e_{2,\beta}(t_2) + \gamma_3 e_{3,\beta}(t_2),$$

from which we can isolate $\Delta v^{(1)}$, $\Delta v^{(2)}$, getting

$$\Delta v^{(1)} = u_{10} + \gamma_2 u_{12} + \gamma_3 u_{13},$$

$$\Delta v^{(2)} = u_{20} + \gamma_2 u_{22} + \gamma_3 u_{23}.$$

All the magnitudes that appear in these two equations, except the scalars γ_2 and γ_3, are three-dimensional vectors. As $\Delta\beta = 1$ has been fixed, the maxima of the performance function corresponds to the minima of $\|\Delta v^{(1)}\|_2 + \|\Delta v^{(2)}\|_2$. Computing the derivatives of this function with respect to γ_2 and γ_3 and equating them to zero, we get a system of two polynomial equations of degree four in the two variables γ_2 and γ_3, that must be solved for each couple of values t_1, t_2 (which are the only free parameters).

To solve this system of algebraic equations we can compute the resultant of the two polynomials, which is another polynomial of degree 16 but with only one variable. The roots of the resultant are the common roots of both equations. We can also proceed in the following way. Write

$$\|\Delta v^{(1)}\|_2 + \|\Delta v^{(2)}\|_2 = \sqrt{Q_1(\gamma_2,\gamma_3)} + \sqrt{Q_2(\gamma_2,\gamma_3)},$$

where Q_1 and Q_2 are second order polynomials in two variables. Now perform a change of variables $(\gamma_2,\gamma_3) \longrightarrow (u,v)$ such that in these new variables Q_1 becomes diagonal with unity coefficients and the uv term of Q_2 is cancelled by using a rotation. Denoting the polynomials in the new variables by $\overline{Q}_1$ and $\overline{Q}_2$, we have

$$\begin{aligned}\overline{Q}_1 &= u^2+v^2+1,\\ \overline{Q}_2 &= b_{20}u^2+b_{02}v^2+2b_{10}u+2b_{01}v+b_{00}.\end{aligned}$$

The conditions of extrema become

$$\begin{aligned}\frac{u}{\sqrt{\overline{Q}_1}}+\frac{b_{20}u+b_{10}}{\sqrt{\overline{Q}_2}} &= 0,\\ \frac{v}{\sqrt{\overline{Q}_1}}+\frac{b_{02}v+b_{01}}{\sqrt{\overline{Q}_2}} &= 0,\end{aligned}$$

and dividing both equations we get

$$\frac{u}{v}=\frac{b_{20}u+b_{10}}{b_{02}v+b_{01}}.$$

From the last equation we can isolate v as a function of u. By replacing in some of the previous ones and squaring, we get a simple polynomial in one variable.

Some numerical computations, to find of the optimal values of γ_2 and γ_3, have been done using this last procedure for computing the minima. First we choose an initial halo orbit. For convenience, we consider the orbit parametrized by an angle, as we did before. We keep the names t_1, t_2 for the corresponding angles. To compute the matrix A_{t_1,t_2}, we must fix the values of t_1 and t_2. When t_1 varies between 0 and 2π, t_2 varies between t_1 and $t_1+2\pi$. For each pair (t_1,t_2) the values of γ_2 and γ_3, corresponding to the maximum of the performance function, are computed and from them $\Delta v^{(1)}$, $\Delta v^{(2)}$, the total Δv and the performance are easily derived.

In figure 11, the optimal values of the performance function (using adimensional units for the velocity) and of the total Δv (in m/s) per unit of $\Delta\beta$, are represented for a halo orbit of z-amplitude 0.15. The different curves of the plots correspond to different values of t_1 (varying in $(0^\circ(30^\circ)360^\circ)$, and on each curve t_2 varies between t_1 and t_1+360°. When the value of the performance function is very small, the total Δv is very large. So, in the right hand side figures we have reduced the vertical range to (700,1100). From the value of the unit of adimensional velocity we can compute Δv knowing the value of the performance. Putting all these plots together we get figure 12, in which the value of t_1 varies in $(0^\circ(1^\circ)360^\circ)$.

From the previous figures it appears that, for a fixed value of t_1, there are, usually, two values of t_2 at which the performance function has a local maximum. This is true except for values of t_1 close to 90° and 240°. Near these two values there are three maxima, as it can be seen in the plots, and even four near $t_1 = 270^\circ$. This fact also happens for other values of β. For the forthcoming figures we have selected only the two "main" maxima, that is, for each value of t_1, the two values of t_2 at which the performance function reaches the largest values.

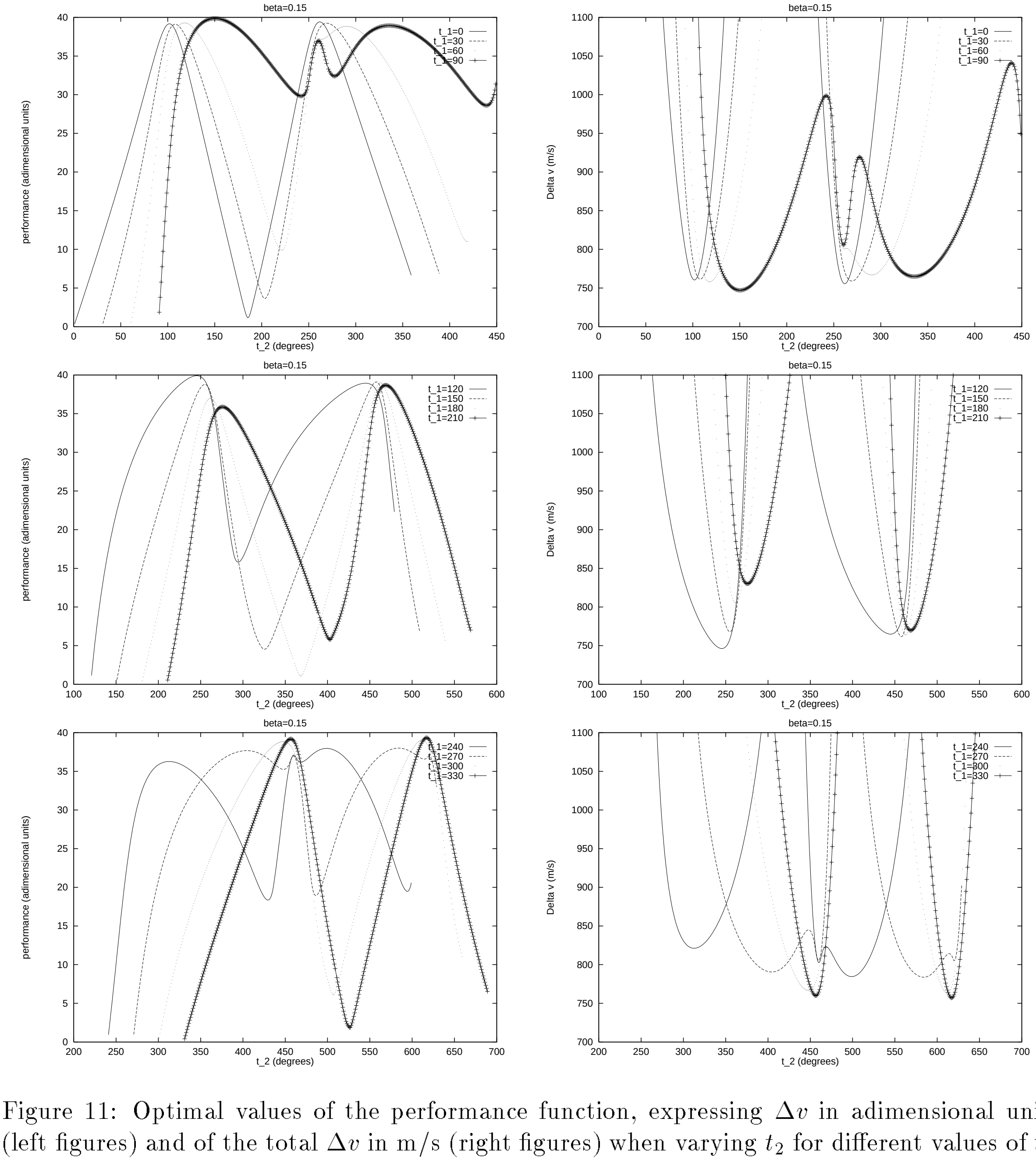

Figure 11: Optimal values of the performance function, expressing Δv in adimensional units (left figures) and of the total Δv in m/s (right figures) when varying t_2 for different values of t_1. The initial halo orbit has $\beta = 0.15$ in all the figures.

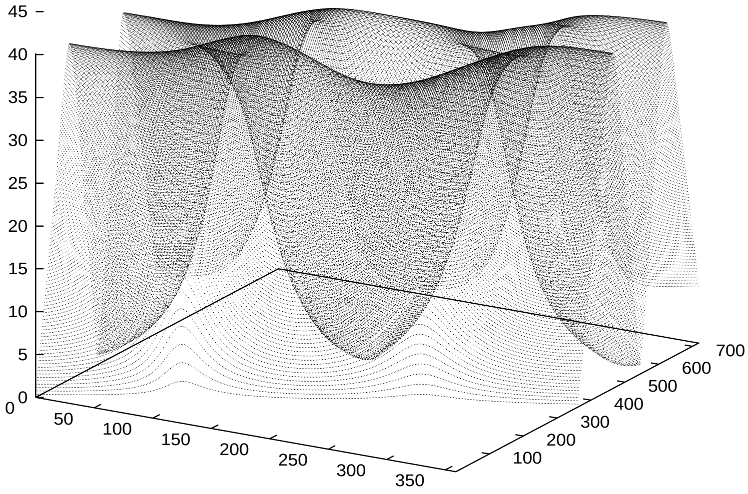

Figure 12: Optimal values of the performance function associated to the values (t_1, t_2) at which the transfer manoeuvres are executed. The computations correspond to an initial halo orbit with z-amplitude β =0.15

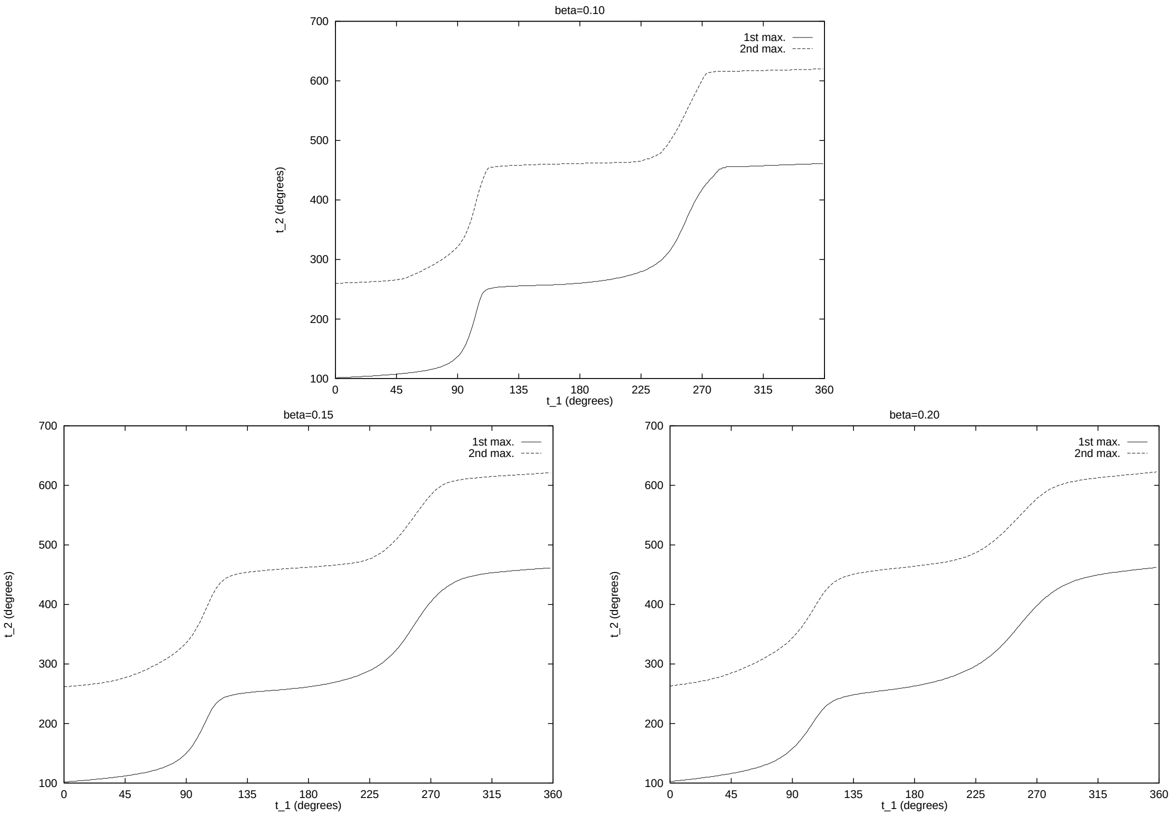

Figure 13: Values of t_2 vs t_1 associated to the optimal values of the performance function for values of β equal to 0.1, 0.15 and 0.20.

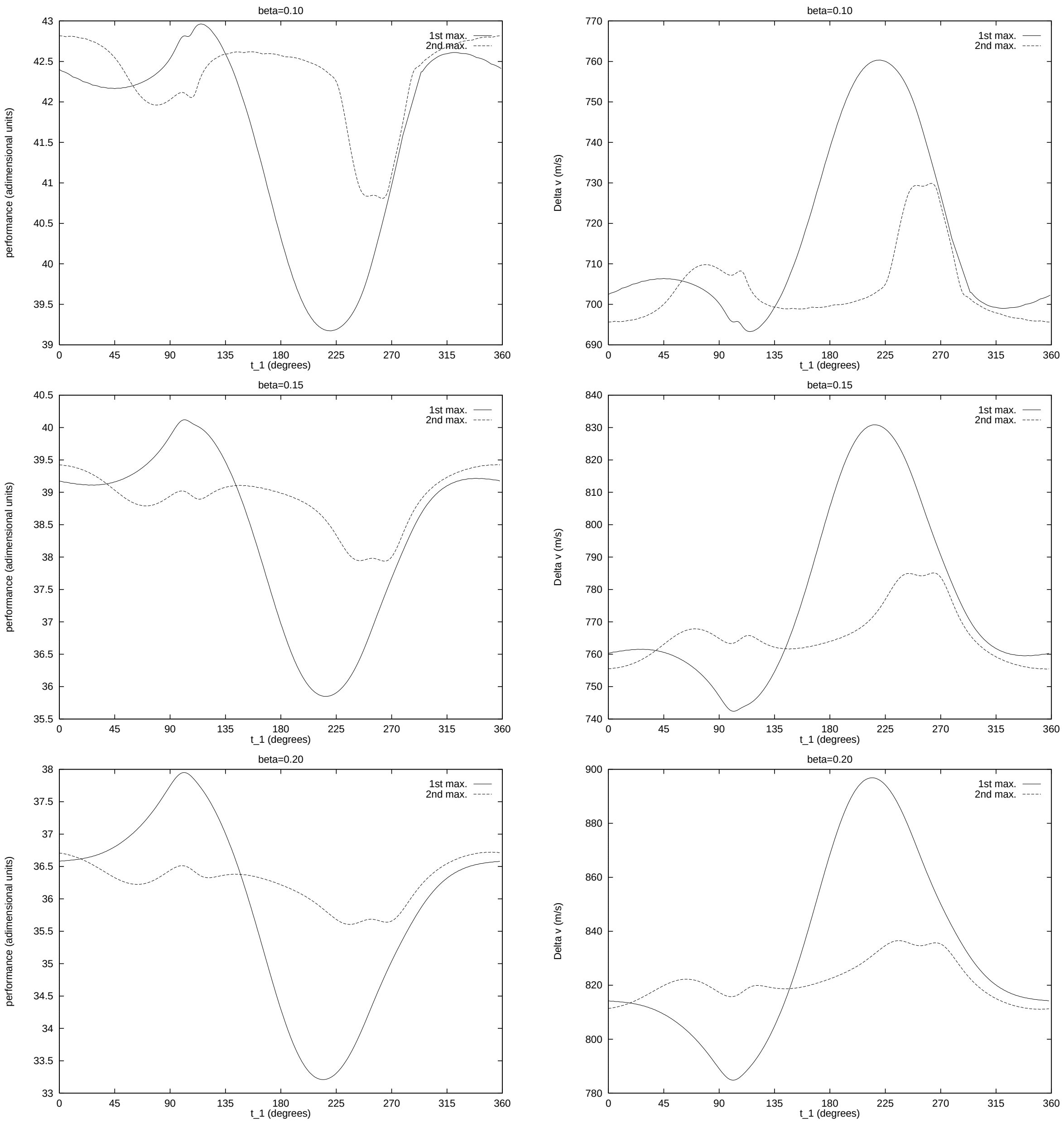

Figure 14: Optimal values of the performance function (left figure) and of the total Δv (per unit of $\Delta\beta$) (right figure) for each value of t_1. From top to bottom, the pairs of figures correspond to an initial halo orbit of amplitude $\beta = 0.1$, 0.15 and 0.20. The values of t_2 related to these extrema, for $\beta = 0.1$, are displayed in the figure 13.

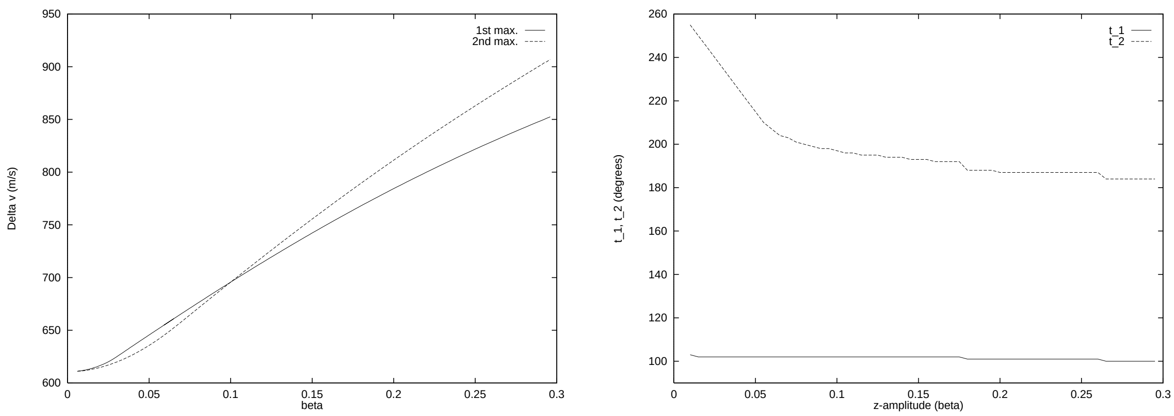

Figure 15: On the left we show the evolution, with β, of the values of the optimal cost in m/s for the two maxima of the performance function. On the right, the values of t_1 and t_2, in degrees, at which the optimal transfer can be done for different values of β, are displayed.

In figure 13 we have represented the optimal values of t_2 versus t_1 for three different values of the z-amplitude. It appears that in all the cases t_2 varies slowly except when t_1 is near 100° and 250°. The difference between the two values of t_2, at which the maximum performance is reached, is almost constant and equal to 180°. That is, after the first manoeuvre has been done, the two optimal possibilities appear separated by a difference of 1/2 of revolution. In figure 14 we show, for these optimal values, the corresponding values of the performance function and of Δv. The cost of the transfer using optimal t_2 is almost constant. The variation around the mean value do not exceeds 4%. If the z-amplitude of the departure orbit is β =0.1, the optimum value is reached using the first maximum for t_1 = 102° and t_2 = 197°. For these particular values, the cost of the transfer, per unit of $\Delta\beta$, is of 696 m/s. The cost increases with β: for β =0.15, the optimal value is Δv = 742 m/s (t_1 = 102°, t_2 = 193°) and for β =0.2 Δv = 785 m/s (t_1 = 101°, t_2 = 187°). The variation with β of the optimal value of the cost is shown in figure 15. It can be seen that this variation is almost linear and that the values of the optimal cost, for the two maxima of the performance function, are very close. In the same figure we have represented the values of t_1 and t_2 at which the manoeuvres must be done. The value t_1 for the first manoeuvre is almost constant and equal to 100°, the corresponding point in the physical space being always very close to the $z = 0$ plane. For very small values of β, the second manoeuvre (the IM) must be done after t_2 = 270°, but this value decreases quickly and for $\beta \in (0.1, 0.3)$ it is of the order of t_2 = 190°, approximately. That is, one has to wait, typically, 1/4 of revolution after the first manoeuvre, to do the second one.

In figure 16 we show the evolution of the transfer trajectories, for the optimal situation mentioned above, taking as departure orbit the one with β =0.1. We have represented the trajectories after multiplying the transfer impulses, computed for a transfer of one unit of $\Delta\beta$, by some scaling factor. Depending on the sign of the factor we increase or decrease the z-amplitude of the departure halo orbit and we reach a final orbit far or close to the departing one. If we decrease the amplitude and the factor is too large, the final orbit is an almost planar one, as is clearly seen in one of the plots (factor=-0.09), in which we start with a halo orbit with $\beta = 0.1$ and we perform a manoeuvre in order to reach another halo with amplitude 0.01. As we are using just a linear approximation of the invariant stable manifold of the orbit, the β value of the initial orbit and not the final one and, furthermore, they are highly unstable, the orbits go away after some time.

In the developed procedure, the departure manoeuvres performed are not requested to have explicitly a tangent to the family component, given by the fourth Floquet mode. We have computed the angle formed by the first manoeuvre at $t = t_1$ and the three velocity components

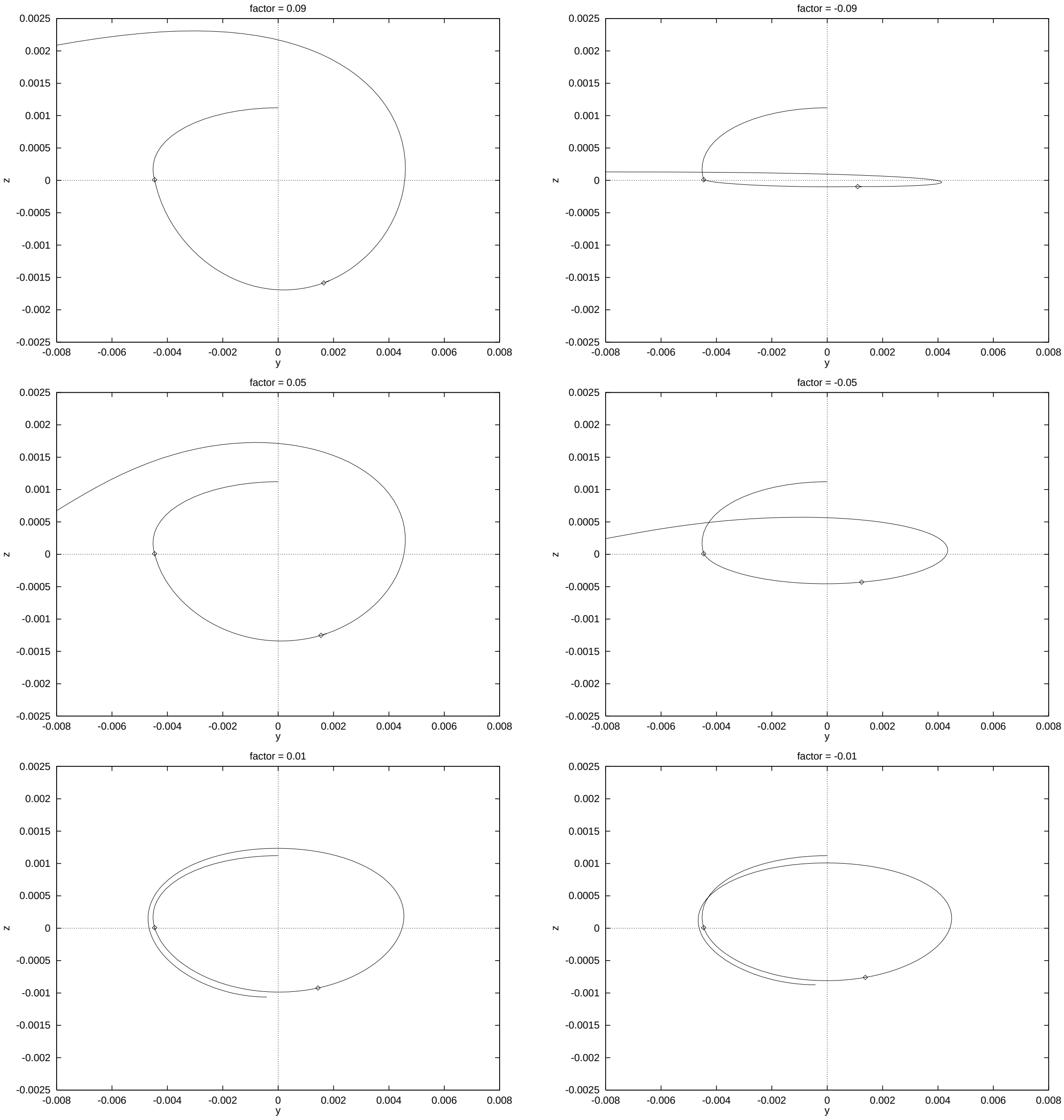

Figure 16: (y, z)-projections (in adimensional units) of the transfer trajectories starting at a departure orbit of z-amplitude $\beta = 0.1$. The manoeuvres have been performed at the two marked points of each plot, which correspond to t_1=102^o=0.86675352 adimensional time units and $t_2 = 193^o = 1.6740240$ adimensional time units. The values of Δv at these two points are equal to $(-0.0030088862, 0.0034410044, -0.020278992)^T \times \mathit{factor}$ and $(0.00014634913, 0.0024107799, 0.00088384102)^T \times \mathit{factor}$. The value of the parameter *factor* varies for the different plots, and has been taken equal to ± 0.09, ± 0.05 and ± 0.01. The integrations have been stopped some time after the second manoeuvre. The highly unstable character of the halo orbits is clearly seen in these evolutions, in which if the *factor* is not small, the errors of the linear approximation are large and produce a fast escape.

of $e_4(t_1)$. The numerical results show that for the optimal transfer (in the linear approximation) this angle varies almost linearly between 11^o and 5^o when β varies between 0.01 and 0.3. So, the first manoeuvre is close to a TFM which produces an increase or decrease of the z-amplitude. This fact suggests that the results using "completely free" values for the first manoeuvre should be not very different from the ones obtained using a TFM as presented in the preceding Sections. Or, equivalently, that the results using a TFM should be almost as good as the ones with complete freedom in the choice of the first manoeuvre.

7 The Nonlinear Problem: A Second Approximation to the Transfer

In the preceding Section we have used the linear approximation of the invariant stable manifolds to compute a first approximation of the transfer between halo orbits. In the real situation we can follow the same ideas but it must be taken into account that the "true" stable manifold of the orbits must be used.

The computation of this 2-dimensional manifold, at least up to a certain distance to the orbit, can be done in different ways. One is by computing the Taylor–Fourier coefficients of the stable manifold up to a given order, using symbolic manipulation (Taylor in one parameter measuring the distance to the orbit, Fourier in the orbital angle). Of course, this must be done for a family of orbits with different amplitudes. Then the results have to be stored in such a way that it is easy to solve the following problem: given a point in the configuration space, identify the invariant stable manifold at which it belongs, or at least, at which it is close enough. This, which in principle can be done with some effort in the RTBP, requires more effort to extend it to a realistic model of solar system, where the system of differential equations is non autonomous and halo orbits depend on two parameters: the z-amplitude, β, and the initial epoch.

Another feasible procedure, but that also needs a large amount of data if we implement it in a realistic situation is this: For a given β we can compute numerically the stable manifold of the corresponding halo orbit. We can represent, using interpolation, the intersections of this manifold with a sheaf of planes transversal to the orbit at different points. The planes of the sheaf can be parametrized by some angle. If u is the variable used for the representation of the intersections of the manifold, we have

$$u = u_1\rho + u_2\rho^2 + \dots,$$

where, ρ is a measure of the distance to the orbit. All the u_i depend on the angle used for the parametrization of the planes, so they can be stored by means of their Fourier coefficients. In this way we can compute a representation of each coordinate of the manifold as a combination of a Taylor and a Fourier expansion depending on the distance ρ and an angle. Of course this must be done for different z-amplitudes. The output is similar to what one obtains by symbolic manipulation, but avoiding the convergence problems at the price of a larger computational effort.

The method that we have implemented does not require the computation of the manifold and can be easily extended to a more realistic model taking into account the effect of the bodies of the Solar System.

From the linear approximation we know, given an initial halo orbit, H_i, of amplitude β_i, the unitary manoeuvres $(\Delta v^{(1)}, \Delta v^{(2)})$ that must be done to reach a halo orbit with amplitude $\beta_i + 1$, as well as the epochs (and the corresponding points in the phase space $p_1 \in H_i(\beta_i)$, p_2) at which the manoeuvres must be performed. If we multiply the unitary manoeuvres by some scaling factor, *fac*, the z-amplitude of the final orbit shall be, approximately, $\beta_i + fac$.

Assume that we have fixed the value of *fac*. Then, starting the numerical integration at $t = t_1$ and doing the two manoeuvres $fac \cdot \Delta v^{(1)}$, $fac \cdot \Delta v^{(2)}$, we can propagate the trajectory until a point, p_3', at minimum distance to the final halo orbit is reached. As this minimum distance can be arbitrarily small, we must stop the integration if the distance becomes smaller than some amount, e.g., 100 km, that we consider as "practical" arrival to the final orbit. This happens at some $t = t_3$. To the point at minimum distance on the final halo orbit, we can associate an angle, α.

With these values we define a point on the linear approximation of the stable manifold of a final halo orbit H_f of amplitude β_f

$$p_3 = H_f(\alpha) \pm d \cdot e_2.$$

$H_f(\alpha)$ is the point of the target halo orbit with angle α, d is a parameter giving the distance, in the configuration space, from $H_f(\alpha)$ to the point p_3 and e_2 is the stable direction at the same angle α, with its first three components normalized to one. The sign $\pm$ is taken to be in the good direction of the stable manifold, in the sense that, of the two possible points, the one selected is the closest one to p_3'. It must be noted that the point p_3 depends on the values of β_f and d, which in a first approximation can be taken equal to $\beta_i + fac$ and to the minimum distance reached by the linear transfer trajectory, respectively.

If ϕ denotes the flow associated to the vector field, $\phi_{t_3,t_2}(p_3)$ will be the image of the point p_3 when t varies (backwards) between t_3 and t_2. Using this notation we define the following function

$$F(\beta_f, d, t_3) = \phi_{t_3,t_2}(p_3) - p_2.$$

We require the first three components of F to be zero. The values of β_f, d, t_3 that fulfil this condition can be computed by an iterative method. For the obtained values, and using the last three components of the above function, we get the manoeuvre that must be done at t_2 in order to reach the new final point (t_3, p_3).

Summarizing: after all the procedure has been done, we have as input data

- An initial amplitude, β_i, for the departure orbit.
- A value of the scaling factor, *fac*, to be applied to the unitary manoeuvres.
- A first manoeuvre performed at t_1 of magnitude $fac \cdot \Delta v^{(1)}$.
- A second manoeuvre done at t_2 and of magnitude $fac \cdot \Delta v^{(2)}$.

and as output data

- A final amplitude, β_f, for the arrival orbit.
- A point, p_3, on the stable manifold of this orbit.
- A distance, d, from the point p_3 to the final orbit.
- An epoch, t_3, of "practical" arrival to p_3.

The role of fac and β_f can be exchanged, so we can fix the amplitude of the arrival orbit and then we get as an output the value of the factor to be applied to the unitary manoeuvres.

In figure 17 we show the (y, z)-projections of some transfer trajectories computed with this procedure. For illustration purposes, we have chosen the same departure orbit as in figure 16 and we have applied the same scaling factors to the manoeuvres. As it is clearly seen from the figures, the behaviour is now much better: after performing the second manoeuvre, the integration was continued for, approximately, one revolution of the final orbit, and there was not observed any exponential escape from this target orbit as it was in the linear case. Of course the unitary cost of the transfer has varied. In the linear case, starting at a halo orbit with $\beta = 0.1$, the cost for a transfer with $\Delta\beta = 1$ was 693 m/s. This value is close to the ones obtained in the nonlinear case if *fac* is small (698 m/s for *fac*=0.01 and 687 m/s for *fac*=-0.01). The two values are not so close if we jump to a more distant orbit: 723, 731, 751 and 885 m/s for *fac*= 0.05, -0.05, 0.09 and -0.09, respectively.

Anyway, the transfer computed with the above procedure is not optimal, especially if the initial and final orbits are not close. This is because the solution given by the linear approximation, that is used as initial guess in the non linear procedure, is not a good approximation when the orbits have very different z-amplitudes. This becomes clear, in some sense, if we plot the different projections of the transfer trajectories. It appears that they have strong bendings at the points where the manoeuvres are applied, denoting that the transfer trajectory is not a very "natural" trajectory of the system.

What we have done is, using the preceding solution as initial guess, to start an standard optimization procedure in order to minimize the total Δv consumption to perform a transfer between two fixed halo orbits. If we fix the initial and final orbit, we have only four free parameters to perform the optimization. We have selected the following ones: t_1, t_2 and the direction of $\Delta v^{(1)}$ (that can be determined by two angles). In figures 18 and 19 we show the three projections of two transfer trajectories that go form $\beta = 0.25$ to $\beta = 0.08$ (figure 18) and vice versa (figure 19)

It has been observed that the cost of the optimal transfer between two orbits, using the described procedure, is essentially the same, independently of the direction used to go from one to the other. We shall give also here the cost of a unitary transfer. For the example shown in figures 18 and 19, this was of 756 m/s, so the real cost for going from one orbit to the other is $(0.25 - 0.08)\times$ 756 m/s = 128.5 m/s. This is better than the results obtained in Section 5 with two JM (see figure 8) but the improvement is small. In fact, for the optimized manoeuvre, the angle of the TFM and the velocity components of $\bar{e}_2$ is near 2^o.

In figure 20 we show the optimal unitary costs for the transfers between different amplitudes. In the upper curve we have always started at a halo orbit with $\beta = 0.25$ and we have computed the unitary costs for going to a halo orbit of amplitude 0.24, 0.23,...,0.05. The other curves correspond to the same quantity computed for initial halo orbits with $\beta = 0.20, 0.15, 0.10$. The angles between the TFM and the velocity components of $\bar{e}_2$ are always small. They range between 14^o and 1^o, decreasing when the initial amplitude, β_i, increases and, for fixed β_i, when the final amplitude, β_f, decreases. As typical examples, $\beta_i = 0.15$, $\beta_f = 0.09$ give $12.^o7$, and $\beta_i = 0.25$, $\beta_f = 0.15$ give $1.^o4$.

For reference purposes we can consider also the following function. Assume we do a long sequence of "infinitesimal" JM to go from β_i to β_f, each one being optimal according to the linear theory of Section 6. That is, we allow for a very large time for the full transfer, doing very small manoeuvres. The total Δv will be the integral between β_i and β_f of the minimum of the two functions plotted in the right part of figure 15. Let

$$F(\beta) = \int_0^\beta \min \Delta v(\beta) d\beta.$$

Then the cost to go from β_i to β_f is $|F(\beta_f) - F(\beta_i)|$. A plot of F is given in figure 21.

On the other hand, the four curves of figure 20 give immediately the corresponding curves of Δv (in m/s) to go from $\beta_i = 0.25$, 0.20, 0.15 and 0.10 (continuous curves from top to bottom) to a β_f given by the horizontal coordinate, as displayed also in figure 21. We plot as dotted curves the corresponding values using the F function. We see that they are extremely close and, in fact, the results with a single JM optimized are better than with the many "infinitesimal" manoeuvres.

This means that the first approach to the transfer problem between halo orbits, presented in Sections 3 to 5 and based on the use of the tangent to the family vector, is already good enough.

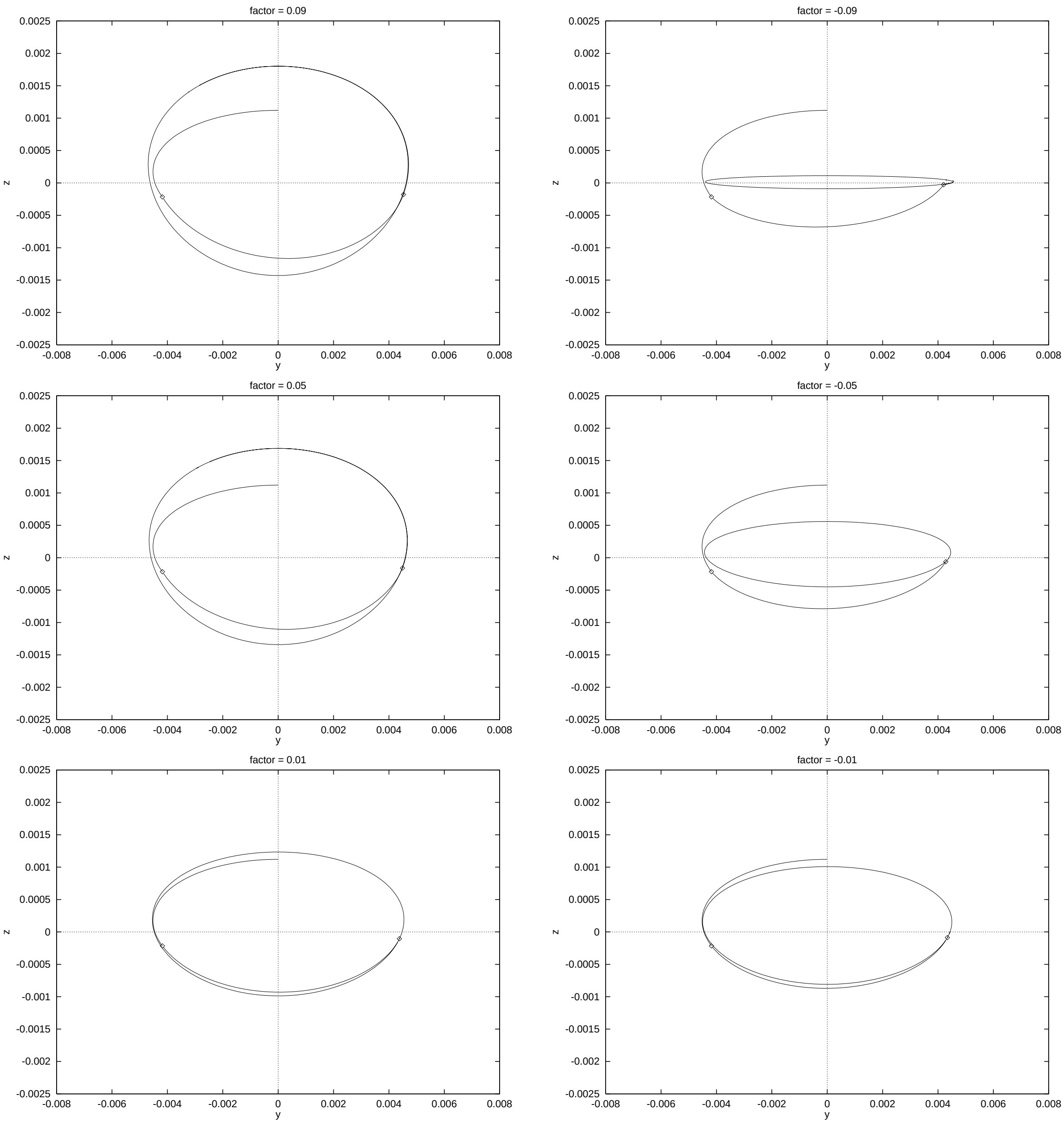

Figure 17: (y, z)-projections (in adimensional units) of the transfer trajectories starting at a departure orbit of z-amplitude $\beta = 0.1$. The manoeuvres have been computed using the nonlinear approximation previously explained. The two marks of each plot correspond to the points at which the manoeuvres have been done. The values of Δv at these two points have been computed multiplying the unitary one by a factor that varies for the different figures as in the linear case. The integrations have been stopped one revolution after the second manoeuvre.

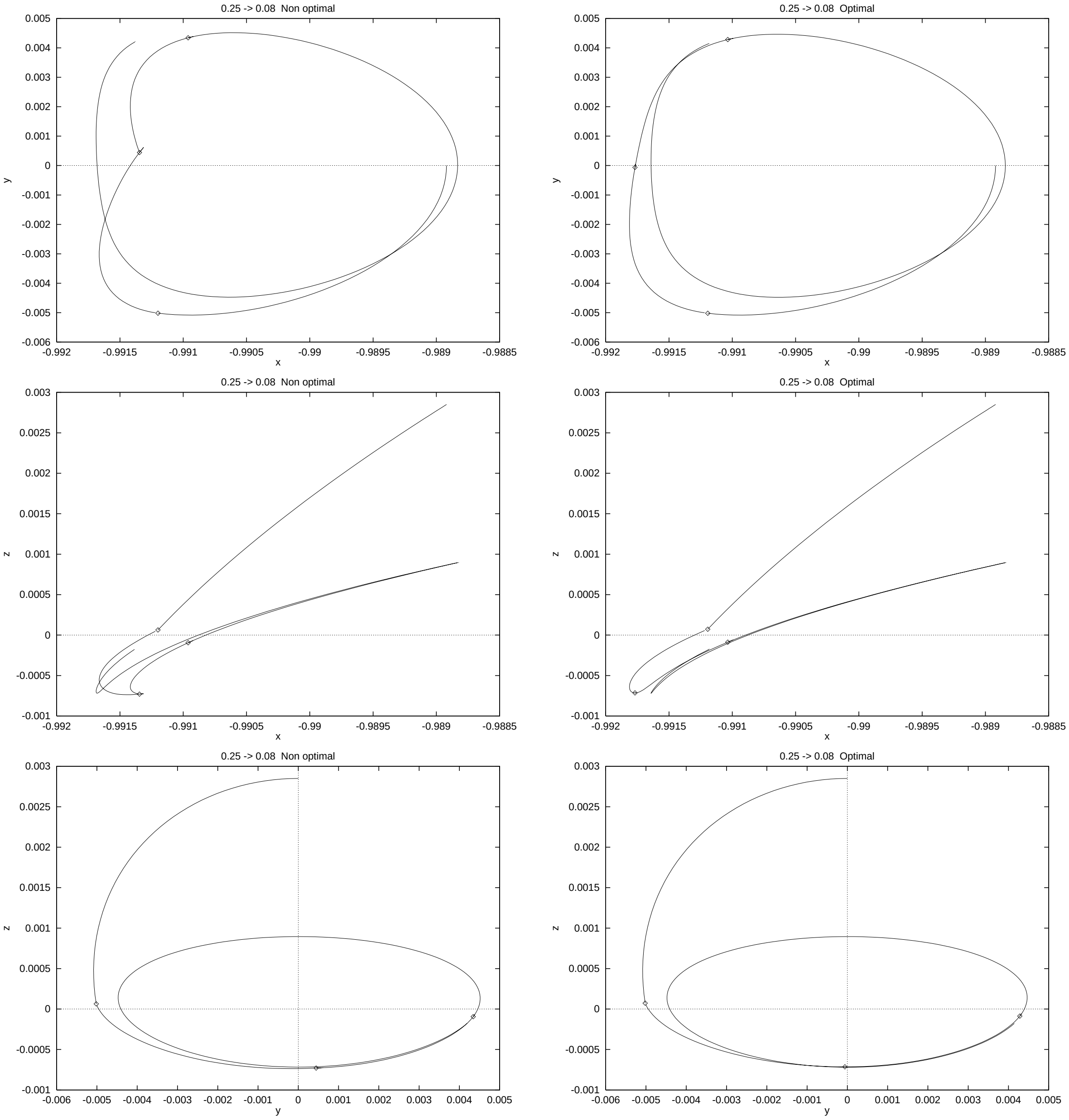

Figure 18: Projections of the transfer trajectories starting at a departure orbit of z-amplitude $\beta = 0.25$ and arriving at a final one with z-amplitude $\beta = 0.08$. The left hand side plots correspond to a non optimal transfer, and the right hand side ones to an optimal one. The three dotted points correspond to the epochs, t_1 and t_2, at which the manoeuvres have been done, and to the epoch, t_3, of minimum distance or "practical" arrival to the final orbit.

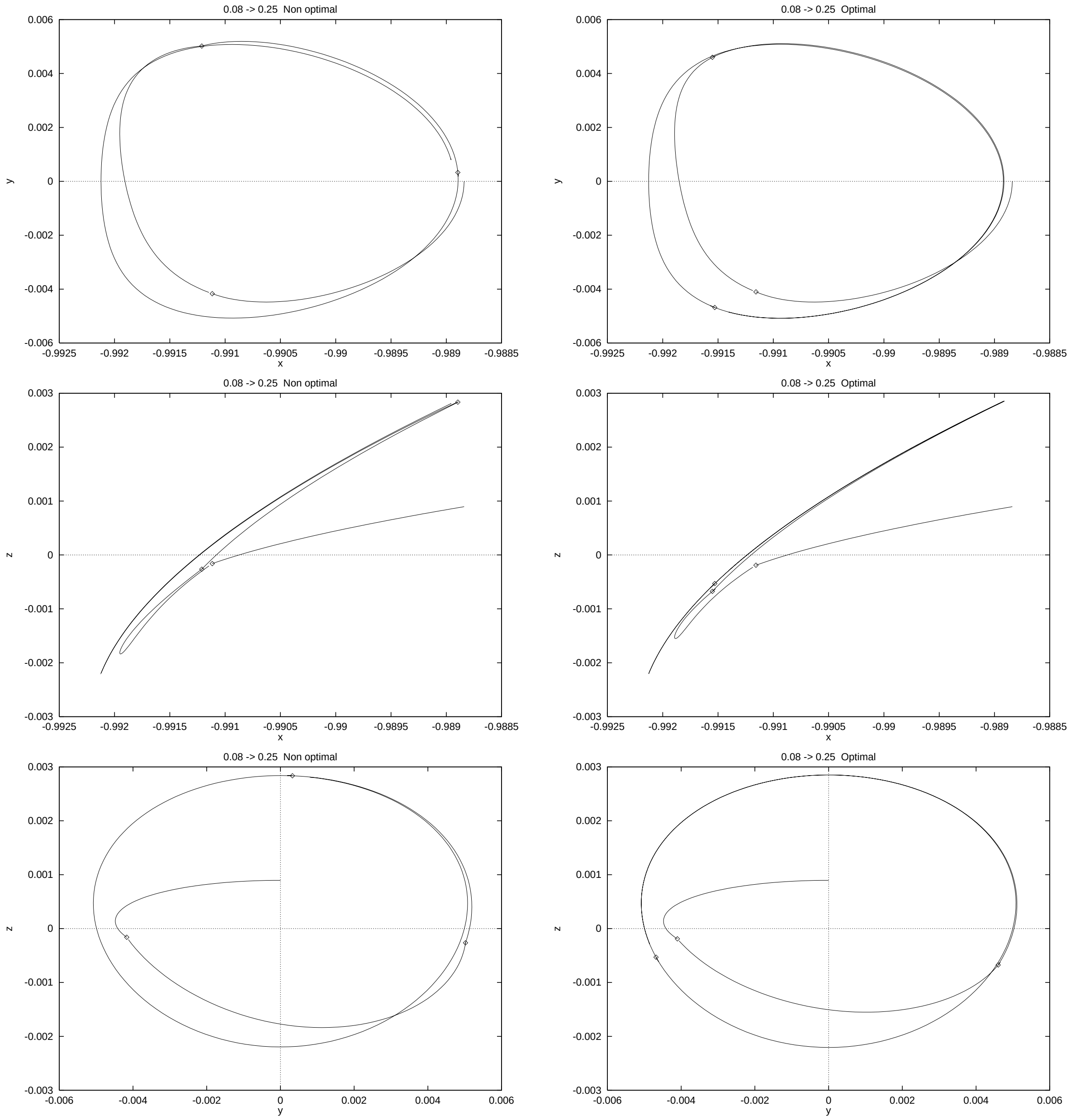

Figure 19: Same as figure 18 exchanging the initial and final values of β.

This justifies why we shall rely mainly on this approach for the extension to the full problem in the next Section.

At this point it is interesting to compare with the Hiday–Howell results. z-amplitudes of 110 000 and 240 000 km correspond to $\beta_i = 0.07345$ and $\beta_f = 0.16026$. From the data of figures 20 or 21 one obtains 63.9 m/s . Hence, we get an improvement of 9% with respect to the Hiday–Howell results.

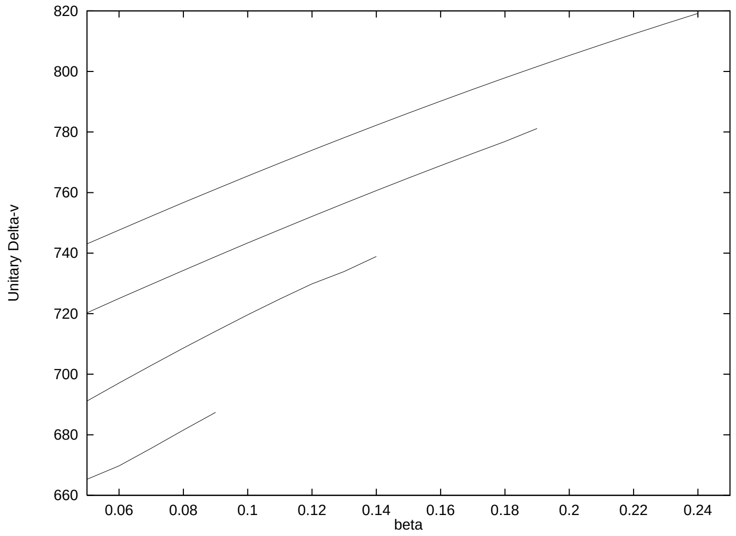

Figure 20: The different curves correspond, from top to bottom, to the optimal values of the unitary costs of a transfer starting at halo orbits with $\beta = 0.25, 0.20, 0.15, 0.10$, respectively, and reaching a final value of β given by the horizontal coordinate in the plot.

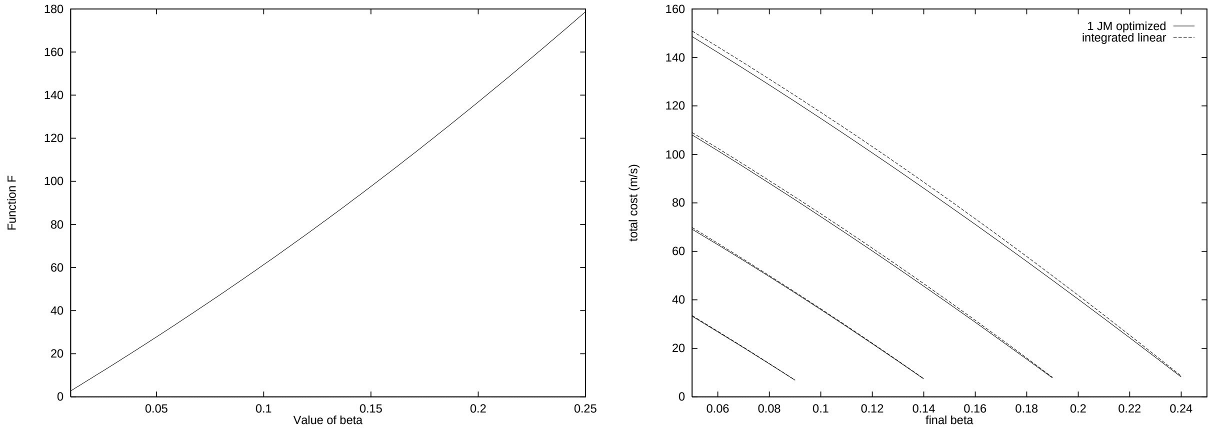

Figure 21: Left: A plot of function F. The difference of values of F between two values of β gives the cost by a sequence of very small JM. Right: The different solid curves correspond, from top to bottom, to the optimal values of Δv of a transfer starting at halo orbits with $\beta = 0.25, 0.20, 0.15, 0.10$, respectively, and reaching a final value of β given by the horizontal coordinate in the plot. The discontinuous curves are obtained as a result of the evaluations using the function F.

8 Extension of the Procedure to the Transfer Between Halo Orbits in the Solar System

The purpose of this Section is to develop a strategy for the transfer in the solar system, similar to the one presented for the RTBP. The main difficulties that appear are due to the non autonomous character of the new vector field and to the near quasiperiodic behaviour of the "new" halo orbits.

Through this Section when we refer to the solar system we consider the force model acting on a spacecraft which takes into account the Sun, the planets and the Moon, all of them considered as punctual masses with their positions and velocities given by JPL ephemeris.

When we consider the equations of motion in the vicinity of the collinear equilibrium points, they can be seen as a perturbation of the restricted three body problem (see [5]). Due to these perturbations the equilibrium points do not longer subsist in the synodic reference frame. They are substituted by geometrical defined ones, using the same relations of the RTBP. Also due to the perturbations, periodic halo orbits do not longer exist in the solar system. They are substituted by quasiperiodic halo orbits which depend not only on initial conditions (position and velocity) but on the epoch, t_0 at which they are given. For their computation different strategies have been used. See [1], [5], [6], and [17] for semianalytical approach and [23] for a pure numerical procedure. All of them using as starting seed a halo orbit of the RTBP.

For the implementation of the transfer in the restricted problem we use the following magnitudes:

- The coordinates of the halo orbits.
- The projection factors in the tangent to the family component.
- The unitary velocity controls, which cancel the tangent to the family component.
- The direction of the stable manifold.

These magnitudes are stored by means of their Fourier coefficients for a net of values of the z-amplitude, and by interpolation they are computed for any value.

When we consider the new quasiperiodic force field all these magnitudes are no longer periodic, so they can not be represented and stored so easily. Moreover they now depend on the z-amplitude and on the initial epoch t_0 used for the computation of the halo orbit.

To deal with these difficulties some simplifications are done. The main one is a consequence of the behaviour of the quasiperiodic halo orbits computed numerically for a certain time span. Keeping fixed the z-amplitude β, the numerical quasiperiodic orbit starting at t_0 and the ones starting at epochs close to t_0 are essentially the same, differing only by a translation in time. So in the computations, the family of quasiperiodic orbits that we consider as the possible nominal ones, have all of them the same epoch t_0 and only the z-amplitude varies. This simplification carries the following problem when computing nominal points.

Recall that in the RTBP, given a state of the spacecraft (position and velocity) to attach a nominal point to it, means to look for a point in the family of periodic halo orbits satisfying a certain condition. The nominal point is characterized by an angle and a z-amplitude. In the new situation, the state of the satellite is given by position, velocity and time, while the nominal point is given by a position and a velocity in a quasiperiodic halo orbit at the same epoch. This means that for computing the nominal point we must look for a quasiperiodic halo orbit, varying the z-amplitude and the initial epoch t_0, in such a way that the position and velocity of a certain point of this orbit, computed at the same time that the one given by the state of the satellite, fulfils the adequate condition (minimum distance,...) for being the nominal one. The role of the angle in the RTBP is now played by the epoch t_0. Due to the simplification in the representation of the family of quasiperiodic halo orbits, we can not vary the parameter

t_0, so in principle, the nominal point could only be searched by varying the z-amplitude. The practical implication is that the computation of a nominal point, which in the RTBP was done computing a zero of a certain function, now should be done computing a minimum of a function with respect the z-amplitude. Numerical experiments show that the minimum is not always clearly defined and its computation is ill conditioned. This has been overcome in the following way.

Given a state of the satellite we assign to it a quasiperiodic halo orbit of a certain z-amplitude, with t_0 fixed, choosing as nominal point the same one as if we were in the RTBP. That is we vary the z-amplitude and we move along the orbit, changing the time t but keeping t_0 fixed. Of course in this way the nominal point will not be right one, since the state of the spacecraft and the nominal point will be related to different epochs. But, as we have explained before, the real nominal point will be very close, in position and velocity, to the one computed. It will be in a quasiperiodic halo orbit with the same z-amplitude but with a value of t_0, shifted by the difference between the epochs associated with the state of the satellite and to the approximated nominal point found.

In principle this method could not be applied if the difference between the epochs of the satellite and the approximated nominal point were too large. Hopefully the difference, as we can see in Table 1, is very small and the behaviour of the approximated nominal point has been good enough for our purposes.

A second simplification can be done if we classify the magnitudes needed for the transfer according to their role. For instance, the coordinates of the halo orbits and their stable directions must be computed very precisely, since from them depend in a critical way the magnitudes related to the control of the satellite. Other magnitudes, such as the the projection factors in the tangent direction, are not so critical and can be computed with less accuracy.

This simplification consists in taking, for the values of the magnitudes related to the tangent impulse, the ones computed for the RTBP, and the true ones for the magnitudes involved in the computations of the insertion in the quasiperiodic halo orbit. The TFM has been done using the second of the strategies described in Section 3. In spite of the fact that none of the procedures is used with the true parameters, the second one has behaved somewhat better.

Taking into account all the above considerations, the jump manoeuvre works in the following way:

1.- Given a state of the satellite in the solar system, $S_{ss}(t) = (S^p_{ss}, S^v_{ss})$, which we assume close to a quasiperiodic halo orbit, we transform it to RTBP coordinates, S_r.

2.- We compute N_r, the nominal point at minimum distance corresponding to S_r.

3.- We perform a change in the velocity components of N_r in such a way that the total Δv used for the TFM is fixed to a given value (selected at will by the transfer designer). We denote this new state as $\bar{N}_r$.

4.- We transform $\bar{N}_r$, at the epoch t to the solar system coordinates obtaining $\bar{S}_{ss}$. If S_{ss} is on a halo orbit, then $\bar{S}_{ss}$, differs from S_{ss} only in the velocity components (leaving aside rounding errors) and $|| S^v_{ss} - \bar{S}^v_{ss} ||_2$ is equal to the Δv used.

5.- We substitute in S_{ss}, S^v_{ss} by $\bar{S}^v_{ss}$. The new state is denoted as $\hat{S}_{ss}$ from now on. Note that the magnitude of the manoeuvre is $\|\Delta v\|$ when the spacecraft is on a halo orbit, and it is slightly different when we are close.

6.- We propagate the state $\hat{S}_{ss}$ in the solar system. At each step of the integration we compute the nominal point at minimum distance, N_m and the nominal point N_w. We remind that last one is the point that can be reached by a manoeuvre inserting into the corresponding stable manifold.

7.- When we reach the maximum of the performance function of the JM, or when we are too far from the family of halo orbits (this can happen due to its highly unstable character) we perform an IM to go into the stable manifold of the nominal orbit H_w. Note that the β amplitude of H_w depends on the initial Δv used in item 3.

8.- We continue the numerical integration till we reach the nominal halo orbit H_w. Then we can go to step 1 and repeat the process till we arrive to a quasiperiodic halo orbit of the desired z-amplitude.

9 Some Numerical Results

In this Section we give a sample of results obtained using the transfer procedure previously described.

In the simulations done we have used as quasiperiodic halo orbits those defined by an initial epoch $t_0 = 16436.0$ mjd and a z-amplitude varying from $\beta = 0.05$ to $\beta = 0.25$, with a step $\Delta\beta = 0.005$. For each orbit we store in a file the position and velocity, in solar coordinates, day by day for a time span of 500 days. Another file stores the six components of the stable direction at the same points. Values for intermediate amplitudes and epochs are then obtained by interpolation.

The first example, summarized in Table 1, corresponds to the transfer orbit obtained after doing a TFM of 5.13 m/s at the epoch 16615.0 mjd for the quasiperiodic halo orbit of z-amplitude $\beta = 0.2$ and $t_0 = 16436$. With this manoeuvre we can reach an orbit of z-amplitude $\beta = 0.1672$

The behaviour is very similar to the one observed for the RTBP, at least for the first days of integration. After then, the introduced simplifications combined with the unstable character of the orbit produce a fast escape. This is not critical if we take into account that the IM must be done about 40 days after the TFM. For this time span the effects of the unstability are not yet critical. It is found that about $T = 16655$ the performance function reaches a maximum. The values of T displayed in Table 1 are just obtained from the integration method, with automatic step size control, starting with a step of 1/2 days and using a maximum step size of 2 days.

In the next two examples we depart from a halo orbit of z-amplitude $\beta = 0.2$ at the epoch 16615.0 mjd and we reach a halo orbit of z-amplitude $\beta = 0.08$. In both examples the IM has been done at the optimal epoch, according to the performance function.

In the first example only one JM has been done. The TFM is of 32.00 m/s at 0^o and the IM of 75.03 m/s is also done near 90^0, approximately 35 days after the TFM. The total cost is Δv =107.03 m/s. Given the initial and final values of β, the size of the TFM should be chosen to reach the desired final β. This determines the size of the IM, too.

In the second one two JM have been done. The TFM are of 5.12 m/s and 13.02 m/s given at 0^o and the corresponding IM are of 23.97 m/s and 46.40 m/s performed near 90^o, approximately 40 days after the tangent impulse. The total cost of the transfer is Δv =88.51 m/s. We note that, in this case, there is freedom in the election of the values of each one of the TFM. Equivalently, the amplitude of the intermediate halo orbit can be fixed at will. The results we have obtained show that the total result is not very sensitive to how we split both TFM, provided they are not extremely different. The addition of more JM do not improves the results in a significative way. This could be expected. Indeed, from the data represented in figure 20 it follows that, in the linear case and using one JM, the total cost in the RTBP to go from $\beta = 0.20$ to $\beta = 0.08$ is 88.14 m/s. Not much better results should be expected for the real case, even using 2 JM.

Figure 22 shows the evolution of the z-amplitude with respect to time of the transfer trajectories, for the two examples. In the plots two z-amplitudes are represented. For each point of the transfer orbit the nominal point at minimum distance, N_m, and the nominal point N_w are computed. The represented amplitudes correspond respectively to those of the orbits H_m

	Nominal Mín. Dist			Nominal H_ω				
T	t	β	D2	t	β	D2	C	P_J
16615.5000	16615.5000	0.1999	0.1387E+02	16615.5000	0.1999	0.1526E+02	5.129	0.1407E−04
16617.3176	16617.3177	0.1993	0.2518E+03	16617.3177	0.1993	0.2759E+03	5.168	0.6539E−04
16619.3176	16619.3177	0.1987	0.6251E+03	16619.3177	0.1987	0.6781E+03	5.232	0.1223E−03
16621.3176	16621.3178	0.1981	0.7429E+03	16621.3178	0.1981	0.8005E+03	5.317	0.1795E−03
16623.3176	16623.3178	0.1975	0.4007E+03	16623.3178	0.1975	0.4228E+03	5.425	0.2373E−03
16625.3176	16625.3179	0.1968	0.2867E+00	16625.3179	0.1968	0.7642E+00	5.559	0.2956E−03
16627.3176	16627.3180	0.1962	0.1161E+04	16627.3180	0.1962	0.1272E+04	5.721	0.3545E−03
16629.3176	16629.3182	0.1954	0.7555E+04	16629.3181	0.1954	0.8199E+04	5.915	0.4143E−03
16631.3176	16631.3183	0.1947	0.2606E+05	16631.3183	0.1947	0.2792E+05	6.144	0.4749E−03
16633.3176	16633.3185	0.1938	0.6833E+05	16633.3185	0.1938	0.7327E+05	6.415	0.5365E−03
16635.3176	16635.3187	0.1929	0.1531E+06	16635.3186	0.1929	0.1647E+06	6.736	0.5993E−03
16637.3176	16637.3189	0.1919	0.3095E+06	16637.3188	0.1919	0.3341E+06	7.116	0.6634E−03
16639.3176	16639.3191	0.1909	0.5821E+06	16639.3191	0.1907	0.6316E+06	7.569	0.7290E−03
16641.3176	16641.3194	0.1896	0.1038E+07	16641.3193	0.1895	0.1135E+07	8.114	0.7962E−03
16643.3176	16643.3197	0.1883	0.1780E+07	16643.3197	0.1880	0.1965E+07	8.776	0.8652E−03
16645.3176	16645.3201	0.1867	0.2966E+07	16645.3200	0.1862	0.3316E+07	9.592	0.9363E−03
16647.3176	16647.3205	0.1848	0.4843E+07	16647.3204	0.1841	0.5514E+07	10.62	0.1010E−02
16649.3176	16649.3210	0.1827	0.7810E+07	16649.3209	0.1815	0.9113E+07	11.93	0.1086E−02
16651.3176	16651.3216	0.1802	0.1253E+08	16651.3216	0.1781	0.1514E+08	13.67	0.1164E−02
16653.3176	16653.3223	0.1771	0.2013E+08	16653.3224	0.1736	0.2557E+08	16.06	0.1246E−02
16655.3176	16655.3230	0.1736	0.3263E+08	16655.3235	0.1672	0.4468E+08	19.53	0.1332E−02

Table 1: Evolution of a transfer trajectory after doing a TFM. T is the true epoch in mjd. t denotes the epoch related to the nominal point. $D2$ is the square of the distance (in km) from the real point to the nominal one. C is the insertion cost (m/s) into the stable manifold and P_J is the performance of the JM.

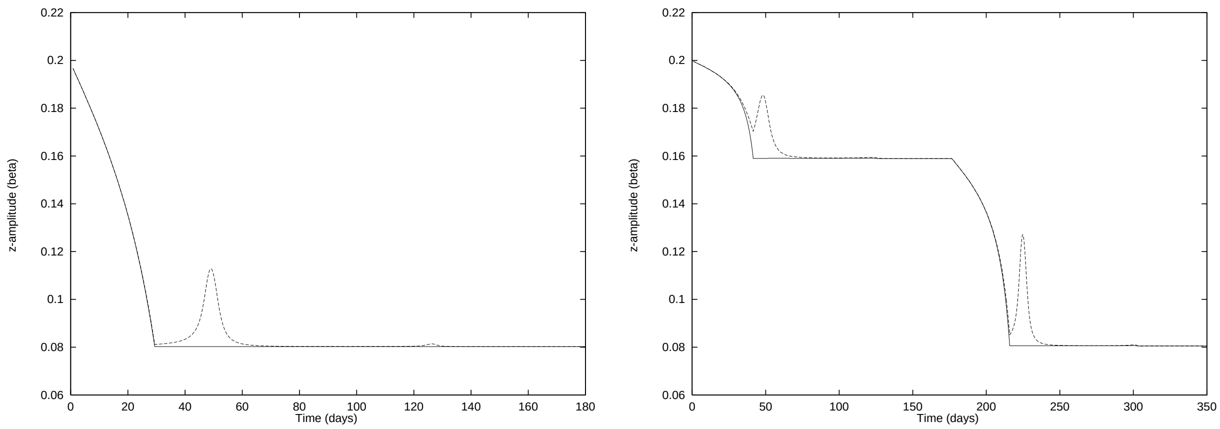

Figure 22: z-amplitude (β) of the nominal orbits with respect to time in days. Solid line, nominal orbit H_w. Dotted line, nominal orbit at minimum distance. Left: Case of one JM. Right: Case of two JM.

and H_w. We note that after performing the IM the z-amplitude corresponding to H_w remains constant until a new TFM is done, meanwhile the z-amplitude related with H_m tends to the constant value after some oscillations.

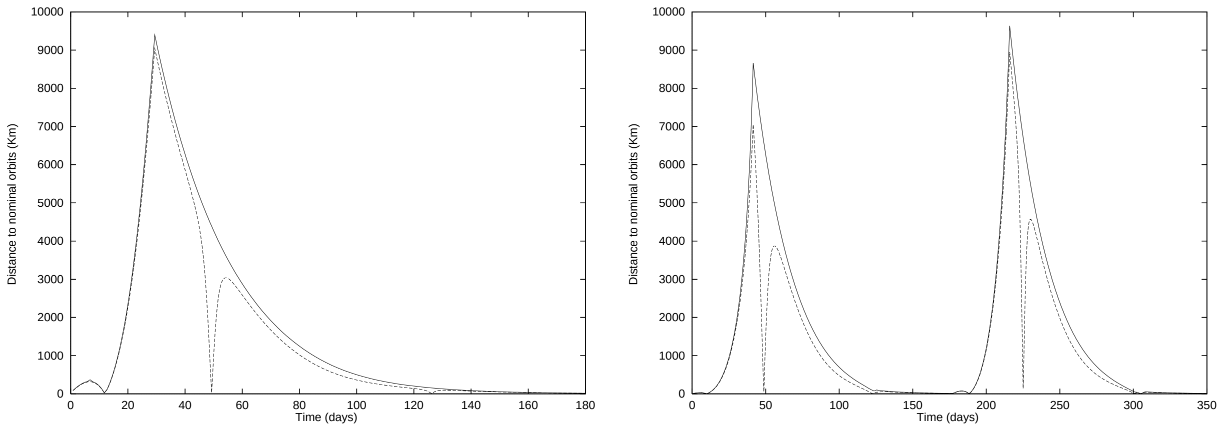

Figure 23: Distance to the nominal orbits in km, with respect to time in days. Solid line, nominal orbit H_w. Dotted line, nominal orbit at minimum distance. Left: Case of one JM. Right: Case of two JM.

In figure 23 we give the distance from the points of the transfer trajectories to the nominal points N_m and N_w, also for the two examples. The behaviour is similar for each JM. We see that after a TFM a fast escape appears until the IM is done (at the maxima of the solid lines). Then the spacecraft tends asymptotically to the nominal point N_w. Of course, the plots of the distance to the N_m points are always below the ones corresponding to N_w.

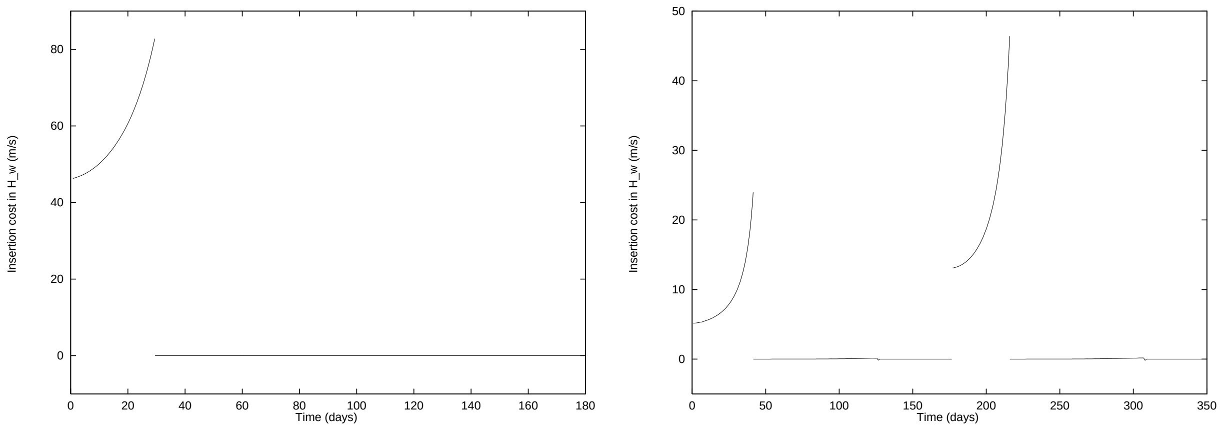

Figure 24: Insertion cost (in m/s) in the nominal orbit H_w in front of time (in days). The jump discontinuities with respect to zero correspond to the manoeuvres performed. Left: Case of one JM. Right: Case of two JM.

In figure 24 we show the insertion cost to H_w with respect to time. Discontinuities correspond to manoeuvres. We note that after a TFM this cost grows whilst after an IM it remains constant and equal to zero since we are tending to the nominal orbit H_w.

Finally in figures 25 and 26 the projections of the transfer trajectories in RTBP coordinates are given for both cases.

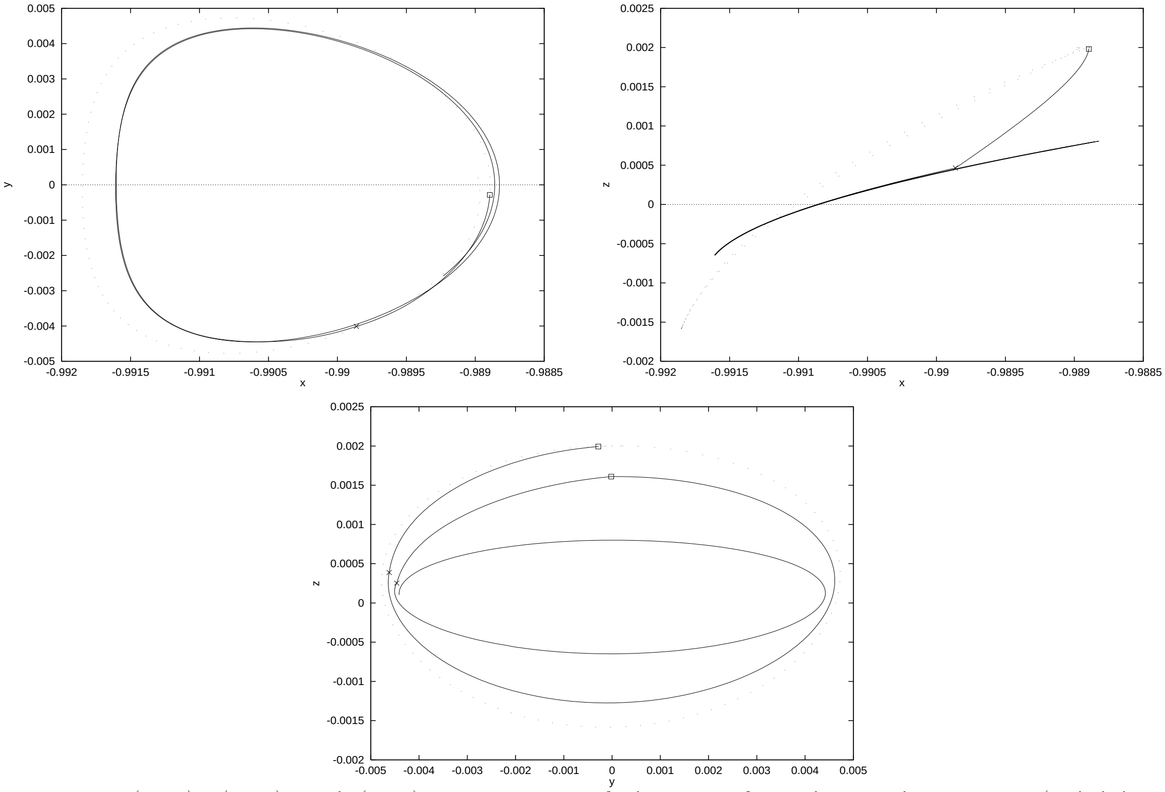

Figure 25: (x, y), (x, z) and (y, z) projections of the transfer orbit with one JM (solid lines) in RTBP variables. The quasiperiodic departure orbit ($\beta = 0.2$) is shown (dotted lines). The points marked with a small box correspond to TFM and those marked with a cross to IM.

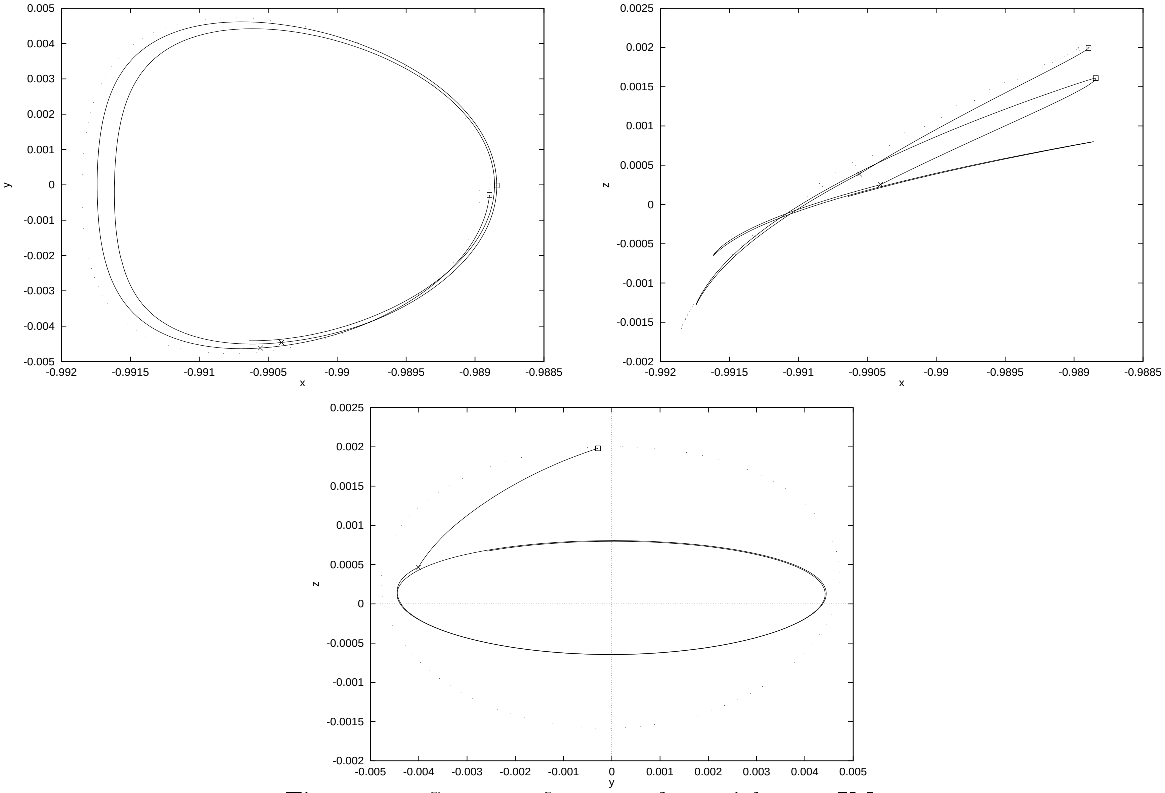

Figure 26: Same as figure 25 but with two JM.

10 Discussion, conclusions and outlook

In this paper we have shown a systematic way of performing transfers between halo orbits of the same family. The dynamics of the motion in a neighbourhood of a periodic halo orbit, allows to establish a natural procedure to perform the transfer. First, a method based on the heuristic idea that the first manoeuvre must be in the *tangent direction to the family of halo orbits* and the second one in the *direction of the stable manifold* at the right epoch to get maximal performance, is used. Later on we allow for general manoeuvres, a detailed analysis of the linear case (nearby initial and target orbits) is done and the nonlinear extension is optimized. We reach very similar results, showing that the heuristic approach is near optimum.

Once the methodology for the RTBP has been set, its extension to a more real situation is rather easy, been the differences between both cases more technical than conceptual.

A careful study of the performance function gives information about the most suitable epochs at which the manoeuvres must be done. The cost of the transfer is then *almost proportional of the difference between the z-amplitudes of the initial and final orbits*, the proportionality constant ranging from $660\mathrm{ms}^{-1}/\Delta\beta$ (when both β_i and β_f are small) to $820\mathrm{ms}^{-1}/\Delta\beta$ (both large, near 0.25). These results systematize and improve by some 9% the previous ones obtained by Hiday–Howell.

The methodology can be extended to the transfer between halo an Lissajous orbits (i.e., orbits on 2D tori in the RTBP model, with two basic frequencies) and between different Lissajous orbits. The differences are technical rather than conceptual. The extensions to the transfer between halo orbits of different families or between halo or Lissajous orbits around different collinear libration points (L_1 and L_2) are also possible. Contributions to those problems are in progress.

Acknowledgements: This work has been supported by DGICYT Grant PB 94–0215 (Spain). Partial support of the EC grant ERBCHRXCT940460, and the catalan grant CIRIT 1996S0GR-00105 is also acknowledged.

References

[1] Díez, C., Jorba, À., Simó, C.: A dynamical equivalent to the equilateral libration points of the Earth-Moon system. *Cel. Mech.* 50 (1991) 13-30.

[2] Eismont, N., Dunham, D., Sho-Chiang, J., Farquhar, R.: Lunar swingby as a tool for halo-orbit optimization in Relict-2 project. *Proc. Third Int. Symp. Spacecraft Flight Dynamics* ESA SP-326 (1991) 435-439.

[3] Farquhar, R.D., Muhonen, D.P., Newman, C., Heuberger, H.: The first libration point satellite. Mission overview and flight history. AAS/AIAA Astrodynamics Spec. Conf., 1979.

[4] Farquhar, R.D., Muhonen, D.P., Richardson, D.L.: Mission design for a Halo Orbiter of the Earth. *J. Spacecraft* 14 (1976), 170-177.

[5] Gómez, G., Llibre, J., Martínez, R., Simó, C.: Station Keeping of Libration Point Orbits, ESOC Contract 5648/83/D/JS(SC), Final Report, 1985.

[6] Gómez, G., Jorba, À., Masdemont, J., Simó, C.: Study Refinement of Semi-Analytical Halo Orbit Theory. ESOC Contract 8625/89/D/MD(SC), Final Report, 1991.

[7] Gómez, G., Jorba, À., Masdemont, J., Simó, C.: Moon's influence on the transfer from the Earth to a Halo orbit. *Predictability, Stability and Chaos in N-Body Dynamical Systems.* Ed. A. E. Roy. Plenum Press 1991, 283-290.

[8] Gómez, G., Jorba, À., Masdemont, J., Simó, C.: A Dynamical Systems Approach for the Analysis of the SOHO Mission, *Proc. Third Int. Symp. Spacecraft Flight Dynamics* ESA SP-326 (1991) 449-454.

[9] Gómez, G., Jorba, À., Masdemont, J., Simó, C.: Study of the Transfer from the Earth to a Halo Orbit around the Equilibrium Point L_1. *Cel. Mech.* 56 (1993) 541–562.

[10] Goudas, C.L.: Three dimensional periodic orbits and their stability, *Icarus* 2 (1963),1-18.

[11] Hénon, M.: Vertical stability of periodic orbits in the restricted problem I. Equal masses, *Astron. Astroph.* 28 (1973), 415–426.

[12] Hechler, M.: SOHO Mission Analysis L_1 Transfer Trajectory, MAO Working Paper No. 202, 1984.

[13] Hiday, L.A., Howell, K.C.: Transfers between libration-point orbits in the elliptic restricted problem. AAS/AIAA Space Flight Mechanics Meeting, Paper AAS 92-126, Colorado, 1992.

[14] Howell, K.C., Hiday-Johnston, L.A.: Time-Free Transfers between Libration-Point orbits in the elliptic restricted problem. *Acta Astronautica* 32 (1994), 245–254.

[15] Huber, M.C.E. et al.: The History of the SOHO Mission. *ESA Bulletin* 86 (1996), 25–35.

[16] Jorba, À., Simó, C.: On Quasiperiodic Perturbations of Elliptic Equilibrium Points, *SIAM J. of Math. Analysis*, 27 (1996), 1704–1737.

[17] Jorba, À., Villanueva, J.: On the Persistence of Lower Dimensional Invariant Tori under Quasiperiodic Perturbations, to appear in J. of Nonlinear Science.

[18] Lawden, D.F.: Optimal Trajectories for Space Navigation. Butterworths & Co. Publishers, London 1963.

[19] Masdemont, J.: Estudi i Utilització de Varietats Invariants en Problemes de Mecànica Celeste, Ph D. Thesis, Universitat Politècnica de Catalunya, 1991.

[20] Richardson, D.L.: A Note on the Lagrangian Formulation for Motion About the Collinear Points, *Celestial Mechanics* 22 (1980), 231-236.

[21] Richardson, D.L.: Analytical construction of periodic orbits about the collinear points. *Celestial Mechanics* 22 (1980), 241–253.

[22] Richardson, D.L.: Halo orbit formulation for the ISEE-3 mission. *J. Guidance and control* 3 (1980), 543–548.

[23] Rodríguez-Canabal J.: Operational Halo Orbit Maintenance Technique for SOHO. *Second International Symposium on Spacecraft Flight Dynamics* ESA SP–255 (1986) 71–78.

[24] Wiesel, W., Shelton, W.: Model control of an unstable periodic orbit. *J. Astronomical Sci.*, 31 (1983) 63-76.

[25] Zagouras, C.G., Kazantzis, P.G.: Three-dimensional periodic oscillations generating from plane periodic ones around the collinear Lagrangian points, *Astroph. Space Science* 61 (1979), 389–409.